

Tu-PM-C1

X-RAY STUDIES OF COMPLEXES OF HIV-1 PROTEASE WITH INHIBITORS. Alexander Wlodawer, Maria Miller and Amy Swain, BRI-BRP, NCI-FCRF, Frederick, MD 21701.

Details of the interactions between substrate-based inhibitors and the target enzyme are necessary for the rational design of drugs in that category. We found crystallization conditions under which a variety of inhibitors of HIV-1 protease form single crystals of their respective complexes. All crystals are isomorphous, space group $P2_12_12_1$, $a=51.7\text{\AA}$, $b=59.2\text{\AA}$, $c=62.45\text{\AA}$. The structure of a hexapeptide analog, with a reduced peptide bond between two norleucines, was solved using molecular replacement. Other complexes, including one with a Phe-Pro sequence, were studied by difference Fourier techniques. Inhibitor binding introduces substantial rearrangement of parts of the enzyme and is crucial to forming subsites in the binding cleft. The movement of the flaps is as large as 7\AA , and the active site pocket decreases in size upon inhibitor binding.

Research sponsored by the National Cancer Institute, DHHS, under contract NO. NO1-CO-74101 with BRI.

Tu-PM-C3

COMPARATIVE MODELING OF PROTEINS IN THE DESIGN OF NOVEL RENIN INHIBITORS Jonathan Greer, Computer Assisted Molecular Design Group. Pharmaceutical Products Division, Abbott Laboratories, Abbott Park, IL 60064.

The renin inhibitors project at Abbott has been developing potent inhibitors for several years. Comparative model building methods were used to construct a three-dimensional model structure of the renin enzyme with inhibitors bound to the active site. The model was employed to develop a general strategy of inhibitor design. It has also been helpful in deciding which modifications to make and in suggesting novel compounds to synthesize. Inhibitors were designed to have high inhibitory potency and specificity for human renin. The size of the inhibitors was reduced with a corresponding decrease in peptide character. The model was used to introduce modifications that enhance metabolic stability, improve oral activity, and vary physico-chemical properties.

Tu-PM-C2

PROGRESS IN THE DESIGN OF ANTI-RHINOVIRUS AGENTS. Adi M. Treasurywala, Computational Section Head, Medicinal Chemistry, Sterling Research Group, Rensselaer, NY 12144 in collaboration with D. Pevear, G. Diana, F. Dutko, M. McKinlay, and M. Rossman.

The human rhinoviruses are members of the picornavirus family. Our efforts in the area of designing agents which block various stages in the replication of this virus group will be reviewed. The availability of crystal structures of inhibitors bound to the virus capsid of HRV14 has made a critical difference to the progress of this project and these collaborative efforts will be briefly reviewed. The impact that computational chemical efforts have had on the project will be stressed.

Tu-PM-C4

COMPUTER-ASSISTED LIGAND DESIGN

Renee L. DesJarlais, Brian Shoichet, Dale Bodian, George L. Seibel, Irwin D. Kuntz, Jr.

Department of Pharmaceutical Chemistry, University of California, San Francisco, CA 94143

We present a computer-assisted method to provide novel candidates for drug design. The process utilizes a rapid and automatic method of locating sterically reasonable of small molecules in a receptor site of known three-dimensional structure combined with a scoring scheme that ranks the orientations by how well they fit the site. This docking procedure is the first step in a two step process to provide candidates that may be novel enzyme inhibitors. A large database of small molecule structures is searched for those molecules that have shape complementary to the receptor structure. This ensures good van der Waals interaction between the receptor and the top scoring molecules, but it is unlikely that any of these molecules will have the appropriate electrostatic and hydrogen bonding properties to interact favorably with the receptor. To the docking procedure, we have added a second step that examines the electrostatic and hydrogen bonding properties of the receptor site. These properties are displayed with computer graphics models and are used to suggest positions where chemical modification of the skeleton structures would be desirable to provide chemical complementarity as well as shape complementarity to the receptor site. At the present time, evaluation of the chemical properties is performed by the chemist. This design technique has been applied to several systems and the results are being tested experimentally.

Tu-PM-C5

ROTATIONAL RESONANCE DETERMINATION OF THE STRUCTURE OF A PHOSPHORYLATED AMINOALKYL PHOSPHINATE INHIBITOR OF D-ALANYL-D-ALANINE LIGASE. A McDermott, F. Creuzet, R. Griffin - MIT, Cambridge, MA 02139. L. Zawadzke, Q. Ye, C. Walsh - Harvard Medical School, Boston, MA 02115.

We have used a newly developed solid-state NMR method, rotational resonance (R2), to establish the structure of an inhibited complex formed upon reaction of D-Ala-D-Ala ligase, ATP, and an amino alkyl dipeptide phosphinate analog. The inhibited complex exhibits a ^{31}P -NMR spectrum which is very different from that expected from a mixture of free inhibitor and ATP. At R2, the spectra show evidence for a strong dipolar coupling between the phosphinate phosphorus and a phosphate ester moiety. From the measured coupling, we obtain a P-P through space distance of 2.7 Å which we interpret to mean that the two species are bridged in a P-O-P linkage, thus proving that the mechanism of inactivation involves phosphorylation of the enzyme-bound inhibitor by ATP.

Tu-PM-C7**STRUCTURES OF DNA TRIPLEXES**

Juli Feigon, Ponni Rajagopal, and Vladimir Sklenar, Department of Chemistry and Biochemistry, University of California, Los Angeles, CA 90024

There is currently great interest in DNA triplexes because of their potential use in antisense repression of gene expression and because of the possibility that intramolecular triplexes may form in vivo. However, the molecular details of these structures and their sequence specificities have not yet been fully elucidated. We have obtained detailed proton NMR results on the DNA triplexes formed from d(GA)₄ and d(TC)₄ as well as sequence variations of these. We will present information on the base pairing schemes, helix structure, stability, and sequence specificity of DNA triplexes.

Tu-PM-C6**MODELING THE BINDING SITE OF THE NUCLEOSIDE TRANSPORTER PROTEIN BY 3D-QSAR**

V.N. Viswanadhan¹, J.N. Weinstein¹, and A.K. Ghose². 1. Natl Cancer Institute, Bethesda, MD; 2. ICN Nucleic Acid Res. Inst., Costa Mesa, CA

The nucleoside transporter is a membrane protein responsible for salvage of nucleosides from extracellular sources. Because of our studies indicating a role for inhibitors of this transporter in treatment of cancer and AIDS (Szebeni, et al., PNAS 86:3842, 1989), we have analyzed a set of nucleoside analogues as ligands for the transporter using the method of 3-dimensional quantitative structure-activity relationships (3D-QSAR). The method begins with conformational analysis of each ligand. Multiple regression is then used to correlate structural features of the ligands with their binding constants for the transporter. The model obtained divides the binding site into six pockets and uses nine independent variables. It fits the observed data with a correlation coefficient of 0.94, a standard deviation of 0.22, and an explained variance of 0.80. Contrary to the literature, the heterocyclic base of the nucleoside is shown to be important, and the binding constant is sensitive to its composition, size, and hydrophobicity. These results will be useful in the rational design of transport inhibitors for treatment of cancer and AIDS.

Tu-PM-D1

MAPPING OF THE LOCAL ANESTHETIC BINDING SITE OF THE NICOTINIC AChR BY SITE-DIRECTED MUTAGENESIS. R. J. Leonard, P. Charnet, C. Labarca, N. J. Vogelaar, L. Czyzyk, A. Gouin, N. Davidson, & H. Lester. Dept. of Biology, 156-29, CALTECH. Pasadena, CA 91125.

We have been examining the interaction of a local anesthetic derivative, QX-222, with the ion channel pore of the muscle AChR, using a combination of mutagenesis, oocyte expression, and electrophysiology. Single channel recording, together with macroscopic voltage-jump relaxations, provide a measure of the residence time of the open channel blocker within the pore. We have found systematic changes in the apparent affinity of the open channel for QX-222 following amino acid substitutions in the proposed M2 transmembrane helix of each of the four subunits of the AChR. Assigning the number 1' to the residue at the cytoplasmic end of the M2 helix, positions 2', 6', 10', 14', and 18' are modelled as forming the lining of the pore. Polar to nonpolar substitutions at 6' decrease QX-222 residence time, while the opposite effect is seen at position 10'. Nonpolar to polar substitutions have the converse effect. The distance between the aromatic and quaternary amine moieties of QX-222 correspond almost exactly to the repeat distance of an alpha-helix. This structural feature is common to many local anesthetic drugs. We propose a model for the binding of QX-222 within the ion channel of the AChR which is consistent with these observations. Supported by: NS11756, NS8083, and Muscular Dystrophy Assn.

Tu-PM-D3

HETEROMULTIMER FORMATION CAN PRODUCE A LARGE NUMBER OF DISTINCT K CHANNELS. McCormack, K¹., Lin, J.W²., Ramaswami, M¹., Tanouye, M¹., Iverson, L³., and Rudy, B². (Intro. by Felice Aull). 1. Calif. Inst. of Technol. Pasadena, CA; 2. NYU Medical Center, N.Y., NY; 3. City of Hope, Duarte, CA.

RNAs synthesized from cloned cDNAs derived from the Sh gene in *Drosophila* produce functional K channels in *Xenopus* oocytes. These channels are an aggregate of probably 4 identical subunits. At least six different RNAs are generated from the Sh gene by an alternative splicing mechanism. Each RNA induces a K channel with distinct kinetic properties. The protein products of these RNAs contain a constant region flanked by diverse amino and carboxy termini. We studied whether new channels are formed when two different RNAs are mixed. We will show data of paired mixtures of three RNAs: 37-4 (amino end: 37; carboxy end: 4), 29-37 and a mutant of 29-4 with a shifted voltage-dependence. We find that injection of mixtures of two different RNAs results in the production of a new channel which must contain subunits derived from the two RNAs. Mixed channels can be formed independently of whether the two types of subunits contain the same amino but distinct carboxy end or viceversa. These channels display novel properties of voltage-dependence, and kinetics of development and recovery from inactivation.

Tu-PM-D2

ELECTROSTATIC ALTERATIONS IN A K⁺

CHANNEL. Roderick MacKinnon, Dept. of Cellular and Molecular Physiology, Harvard Medical School, Boston, MA.

Shaker K⁺ channels, when expressed in *Xenopus* oocytes, are susceptible to block by charybdotoxin (CTX). CTX inhibits K⁺ channels by physically plugging the externally facing conduction pore entryway. The toxin is thus a convenient probe to identify protein domains that comprise the outer mouth of the Shaker K⁺ channel. CTX is a highly cationic molecule and therefore charged amino acid residues on the ion channel near the CTX binding site should influence the binding energy. Acidic residues in several regions of the Shaker K⁺ channel were mutated to neutral and cationic residues and the effect of the mutations on CTX inhibition was assessed. One region of the channel, in the relatively hydrophilic segment connecting S5 and S6, appears to be near the CTX binding site and channel outer mouth. Charge alterations involving position 422 (Sh H4) in this region influence CTX block by a simple through-space electrostatic mechanism: as the charge is made more positive the CTX blocking affinity is lowered and the ionic strength dependence of block is diminished. Further experiments designed to identify and characterize residues forming the outer mouth of the channel are currently in progress.

Tu-PM-D4

STRUCTURE-FUNCTION STUDIES ON THE SHAKER K⁺ CHANNEL. E.Y. Isacoff, Y.N. Jan and L.Y. Jan. HHMI, UCSF, San Francisco, CA, 94143. (Intro. by R.M. Stroud)

Shaker and several related K⁺ channel genes code for proteins that are similar in size and predicted transmembrane topology to each of the four internally homologous domains of Na⁺ and Ca²⁺ channels. We have asked whether, by analogy with the pseudo-tetrameric nature of Na⁺ and Ca²⁺ channels, several Shaker polypeptides co-assemble to form multi-subunit channels. The approach has been to see if channels with hybrid inactivation kinetics are produced when *Xenopus* oocytes are coinjected with RNAs from wild-type and mutant alternative-splice products of the Shaker gene, which individually produce channels with distinct kinetics.

Coinjection was first done using RNA from ShA, which shows rapid mono-exponential inactivation, mixed with RNA from an amino-terminal deletion mutant of ShB (ShB17), that was found to eliminate fast inactivation. This mix produced macroscopic currents which inactivated more slowly, and recovered more quickly than ShA. Neither inactivation onset nor its recovery could be described as a linear sum of ShA and ShB17 currents, indicating interaction at the molecular level. Similar effects were seen with tandem "dimers" of ShA and ShB17 linked into a single open reading frame, though the relative amplitudes of the components of inactivation differed. Similar results were obtained with ShA and wild-type ShB. These results indicate that the Shaker K⁺ channel is a multimer and that co-expression of alternative-splice products of the gene may give rise to channels with distinct properties. The finding that tandem constructs produce functional channels supports models that place the amino and carboxy terminals on the same (probably cytoplasmic) side of the membrane.

Tu-PM-D5

SITE-DIRECTED MUTAGENESIS OF THE S4 SEQUENCE OF THE *SHAKER* K⁺ CHANNEL. D. Papazian*, L. Timpe, Y.N. Jan & L. Jan. HHMI, UCSF, San Francisco, CA, 94143, & *Dept. of Physiology, UCLA, Los Angeles, CA 90024. (Intro. by Ronald Vale)

The *Shaker* K⁺ channel contains an S4 sequence similar to those in Na⁺ and Ca²⁺ channels. S4 sequences, which consist of repeated triplets of one basic (arginine or lysine) and two hydrophobic amino acids, have been proposed to function as transmembrane voltage sensors. To test this hypothesis, the S4 arginines and lysines of the *Shaker* cDNA clone, ShB, have been altered by site-directed mutagenesis. The S4 basic amino acids have been replaced one at a time by the neutral amino acid glutamine, or by the other basic amino acid. Mutant channels have been expressed in *Xenopus* oocytes and analyzed by the two electrode voltage clamp method.

Two mutations eliminated channel activity, whereas twelve others conducted A-type currents. A number of these mutations affected the voltage-dependence of the channel, shifting the peak conductance-voltage and steady state inactivation-voltage relationships in parallel along the voltage axis, primarily in the depolarized direction. The slopes of these curves were shallower in two mutants. In mutants with shifted activation and inactivation, the voltage-dependence of the rate of the major component of macroscopic inactivation was also shifted. None of the mutations altered the K⁺ selectivity of the channel, or its rate of recovery from inactivation. These results indicate that the S4 sequence is important for the voltage-dependence of the K⁺ channel.

Tu-Pm-D7

STRUCTURAL AND FUNCTIONAL ANALYSIS OF THE VOLTAGE GATED SODIUM CHANNEL. A.L. Goldin¹, V.J. Auld², T. Hebert², D.S. Krafte³, W.A. Catterall⁴, H.A. Lester⁵, N. Davidson⁵, and R. J. Dunn². ¹Dept. Molecular Genetics, U.C. Irvine, CA, 92717, ²Dept. Neurology, Montreal General Hospital, Quebec H3G 1A4, ³Sterling Research Group, Rensselaer, N.Y. 12144, ⁴Dept. Pharmacology, U. Washington, Seattle, WA 98195, ⁵Dept. Biology, Caltech, Pasadena, CA 91125.

We have reported previously the isolation of a rat brain cDNA encoding an α subunit of the voltage-gated Na⁺ channel (Auld et al., *Neuron* 1:449-461, 1988). Although this α subunit, rat IIA, differs at only 7 amino acid positions from the reported rat II sequence of Noda et al. (*Nature* 320:188-192, 1986), rat IIA channels expressed in *Xenopus* oocytes displayed a current-voltage relationship that was shifted 20-25 mV in the depolarizing direction. To identify those residues responsible for this effect, each of the 7 variant residues in rat IIA has been modified to the corresponding residue in the rat II sequence. We find that a mutation from a leu to phe in the S4 segment of domain II in rat IIA is responsible for the observed voltage shift. Reversion of this single mutation is sufficient to shift the current-voltage relationship back to that seen for channels expressed from rat brain poly(A) RNA or from rat II cDNA, and to increase greatly the number of functional channels in the injected oocytes. We have now made additional mutations in the S4-S5 region of domain II, and found that these also change the current-voltage relationship in unexpected ways that will be discussed.

Tu-PM-D6

MUTAGENESIS OF SHAKER POTASSIUM CHANNELS: WHAT'S BEHIND THE ZIPPER ?

K. McCormack[^], B. Rudy[¶], M. Ramaswami[^], M. K. Mathew[^], L.E. Iverson[§], T.J. McCormack[¶], & M. Tanouye[^] (Intro. by X.C. Yang). [^]Division of Biology, Cal. Tech., Pasadena, Ca 91125, [¶]Department of Physiology, NYU Medical Center, New York, NY 10016, [§]Division of Neurosciences, City of Hope, Duarte, CA 91010.

We have found a leucine-heptad repeat which is well-conserved among all *Shaker* family potassium channel sequences and is located immediately adjacent to the putative voltage-sensing S4 domain. Similar motifs are found in sodium and calcium channels. Following from recent work on dimerization in a class of DNA-binding proteins, the presence of this "leucine-zipper" motif in potassium channel sequences suggests a site for channel subunit interactions. The location of the leucine-zipper motif, next to the S4 domain, would further suggest that voltage-dependent translocation of S4 could alter channel subunit interactions through the leucine-zipper motif. Thus, both structures would be central in determining open and closed states of the channel. To test this notion, we have constructed mutations of a *Drosophila Shaker* transcript within the zipper motif and tested in the *Xenopus* oocyte expression system. We have found that single conservative substitutions have dramatic effects on *Shaker* channel function suggesting that the leucine-zipper motif is, indeed, critical for proper channel function.

Tu-PM-D8

DESIGN, SYNTHESIS, AND FUNCTIONAL EXPRESSION OF A K⁺ CHANNEL GENE.

S.F. Hausdorff, E.E. Rushin and C. Miller. Grad. Dept. of Biochemistry, Brandeis University, Waltham, MA 02254.

A gene that is responsible for a voltage-dependent, potassium-selective ion conductance has recently been cloned from rat kidney mRNA and expressed in *Xenopus* oocytes (Takumi et al., *Science* 242:1042 (1988)). The protein encoded by this gene is a putative potassium channel of only 130 amino acids and a single membrane-spanning region. We have taken advantage of the small size of the gene to synthesize it de novo from synthetic oligonucleotides, thereby introducing a large number of unique restriction sites to facilitate site-directed mutagenesis. Run-off transcripts were made from the synthetic gene, and the mRNA injected into oocytes. The cells were voltage clamped at two days post-injection. In spite of our profligacy in flouting the frequencies of codon usage, oocytes produced large currents which were slow, voltage-dependent, and potassium-selective, as anticipated for this channel. We now have a powerful system for probing the molecular properties of the potassium channel, and are currently expressing the gene in the baculovirus high-level expression system for eventual purification of the channel protein.

Tu-PM-D9

TOTAL SYNTHESIS, EXPRESSION, AND FUNCTIONAL ASSAY OF A GENE ENCODING A HUMAN DELAYED RECTIFIER POTASSIUM CHANNEL R. Swanson, K. Folander, C. Bennett, J. Antanavage, R.B. Stein, and J.S. Smith, Merck Sharp and Dohme Research Labs, West Point, PA

To facilitate structure-function studies, a gene encoding the human I_{K} K^+ channel was chemically synthesized. The gene encodes the native amino acid sequence of the protein but was designed to maximize the number of unique restriction enzyme sites in the nucleotide sequence. The gene is 424 bp long and was assembled from 10 overlapping oligonucleotides. Injection of RNA transcripts of the gene into *Xenopus* oocytes resulted in the expression of a time- and voltage-dependent K^+ current that was recorded using a standard two microelectrode voltage clamp. The current activated slowly at voltages > -25 mV, showed no inactivation during 2s pulses, and was indistinguishable from those elicited by the wild type gene. The nucleotide sequence of our cloned wild type gene differed, however, at one position from the published sequence (Murai, *et al.*, 1989) resulting in a glycine at position 38 instead of the reported serine. Both the Ser³⁸ and Gly³⁸ alleles induced delayed rectifier type K^+ currents in oocytes. The use of the synthetic I_{K} gene will facilitate systematic structure-function studies of this channel by the introduction of mutations using synthetic restriction fragments containing any desired change.

Tu-PM-E1

USING OPTICAL TWEEZERS ON KINESIN-COATED BEADS MOVING ALONG MICROTUBULES. S.M. Block^{†‡}, L.S.B. Goldstein[‡], and B.J. Schnapp[§], [†]Rowland Institute, Cambridge, MA 02142, [‡]Dept. Cell. & Dev. Biology, Harvard University, Cambridge, MA 02138; [§]Dept. Physiology, Boston U. Med Ctr., Boston, MA 02118.

Movement of microscopic beads along microtubules *in vitro* provides a system with unique advantages for investigating kinesin-based motility. We have combined optical trapping technology with an *in vitro* motility assay, an approach that improves the efficiency of this assay to the point where it can work at low kinesin/bead ratios. A gradient force optical trap was used to capture and manipulate coated beads. By steering the laser, beads were deposited directly onto sea urchin axonemes. Movement is rarely produced from random collisions of diffusing beads with microtubules, even when beads are incubated with moderate levels of kinesin (>100 kinesins/bead). However, nearly all beads that were deposited on axonemal microtubules, then released, moved smoothly to the end of the axoneme. Under such conditions beads generate sufficient force to move through the trap without obvious reduction in speed, opposing a force estimated at $\sim 5 \times 10^{-8}$ dyn. Assuming ~ 10 -100 kinesins/bead and that ~ 1 -50 interact with the microtubule, the force per kinesin is ~ 1 -50 $\times 10^{-9}$ dyn. Beads incubated at lower kinesin/bead ratios dissociated from the axonemes after moving short distances (~ 0.5 -2.5 μ m); the distance decreased with lower kinesin/bead ratios. At ~ 10 kinesins/bead, <10% of the beads moved; the longest movement was <0.5 μ m. Application of the trap during movement at the lowest kinesin/bead ratios ripped the bead off the substrate. These results suggest that a kinesin molecule may be incapable of moving a bead for more than a few μ m before either thermal motion or an external force causes dissociation from the microtubule. A videotape will be shown demonstrating the technique.

Tu-PM-E3

SMOOTH MUSCLE CROSSBRIDGE INTERACTIONS MODULATE ACTIN FILAMENT VELOCITY IN VITRO.

D. Warshaw and K. Trybus*; Univ. of Vermont, Burlington, VT; Brandeis Univ., Waltham, MA.

The motion of fluorescently labelled actin on antibody stabilized, smooth muscle myosin filaments adhered to a coverslip was quantitated. Actin filament velocity depends on the proportion of phosphorylated to unphosphorylated crossbridges (XBs) within the myosin filament, suggesting that weakly bound unphosphorylated XBs impede rapidly cycling phosphorylated XBs. To further test this hypothesis, skeletal muscle myosins modified with pPDM and NEM (weak and strong binding analogues, respectively), were copolymerized with phosphorylated smooth and skeletal muscle myosins. Only 1% NEM myosin copolymerized with either smooth or skeletal muscle myosin was needed to completely inhibit actin filament motion. Using the weakly bound analog, as little as 10% pPDM myosin copolymerized with skeletal muscle myosin slowed actin filament velocity, whereas, 75% pPDM myosin had to be copolymerized with smooth muscle myosin before actin filament motion was affected. Therefore, weakly bound XBs can impede faster cycling XBs, which may explain why actin filament velocity depends on the extent of light chain phosphorylation. Phosphorylated smooth muscle XBs may spend more of their cycle time in a strongly bound state compared to fast skeletal muscle myosin since it is more difficult to impede smooth muscle myosin XBs. (Support: NIH HL35864 to DW, HL38113 to KT).

Tu-PM-E2

BIDIRECTIONAL MOVEMENT OF FLUORESCENTLY LABELED ACTIN FILAMENTS ON SINGLE THICK FILAMENTS FROM CLAM MUSCLE

James R. Sellers* and Bechara Kachar*, NHLBI and *NIDCD, NIH, Bethesda MD 20892 (intro. by Larry Miller)

We have isolated native thick filaments from the clam catch and striated muscles by the method of Yamada *et al.* (*J. Muscle Res. and Cell Motil.* 10, 124, 1989) which are 10-40 μ m in length. The movement of rhodamine phalloidin-labeled actin filaments on individual native thick filaments can be observed by a combination of video enhanced DIC microscopy to image the thick filaments and fluorescence microscopy to image the actin filaments. A single segment of thick filament can move actin filaments in both directions. On a number of occasions it was observed that a particular actin filament travels along a thick filament in one direction and then loops back upon itself and travels back in the other direction at approximately the same speed. In these cases it can be seen that the polarity of the actin filament determines the direction of movement. Using native thick filaments isolated from the catch muscle of the clam a bimodal distribution of velocities is observed in the presence of pCa 4.5. Some of the filaments move at with a mean rate of 0.31 μ m/s and others move with a mean rate of 3.81 μ m/s. In many cases, a single actin filament can move first at the slow rate and then at the fast rate or *vice versa* while apparently attached to the same thick filament. Several actin filaments can exhibit this behavior along a single thick filament and the point at which the rates of movement change is the same for each actin filament traveling along the thick filament.

Tu-PM-E4

TRANSPORT OF STRIPPED VESICLES BY MYOSIN I FROM ACANTHAMOEBA H.G. Zot, S.K. Doberstein, and T.D. Pollard Dept. of Cell Biology and Anatomy, The Johns Hopkins University School of Medicine, Baltimore MD 21205

We have reconstituted complexes of myosin-I (MI) with cellular membranes or plastic beads and measured high velocity movements along filament bundles from *Nitella* (Sheetz and Spudich, *Nature* 1983). MI binds to *Acanthamoeba* membranes stripped of peripheral membrane proteins (Adams and Pollard, *Nature* 1989) and these complexes move along the actin bundles 1 to 3 μ m/s. The movements occur in bursts of <200 μ m at irregular time intervals or along zigzag paths for longer distances. Polystyrene beads coated with rabbit muscle myosin translated steadily in the same direction as these bursts at 0.5 μ m/s. While MI coated beads moved slowly (<0.1 μ m/s), beads coated with rabbit F-actin moved steadily for several minutes at approximately the same rate as the stripped vesicles in the presence of MI. The slower velocity of MI coated beads and the irregular movement of the MI-membrane complex may result from the interaction of the ATP-insensitive actin binding site on the tail of MI with the actin bundles. Thus, we measured velocities of complexes containing MI that are 10 to 100 times greater than other reported motile preparations of MI, are consistent with a high ATPase rate, and establish a basis for MI powered transport in the cell. This work was supported by grants from the NIH and AHA Florida Affiliate (GM26132-12 and 88G-514).

Tu-PM-E5

MECHANISM AND REGULATION OF ACTIN FILAMENT TRANSLLOCATION *IN VITRO* BY 110K/CALMODULIN, A VERTEBRATE MYOSIN I Kathleen Collins, James R. Sellers* and Paul Matsudaira, Whitehead Institute, Cambridge, MA 02142 *Laboratory of Molecular Cardiology, NHLBI, NIH, Bethesda, MD 20205.

A complex of 110K-protein and calmodulin directly connects actin to the apical and basolateral membranes of intestinal epithelial cells. The 110K complex, when immobilized on nitrocellulose-coated coverslips, translocates actin filaments at 37°C at a rate of 0.07 to 0.1 $\mu\text{m/s}$. Actin activates the MgATPase activity greater than 40-fold with simple-hyperbolic kinetics, with a K_m of 20-40 μM and V_{max} of 0.86 s^{-1} . Micromolar calcium modestly increases both motility and actin-activated MgATP hydrolysis. Higher concentrations of calcium completely inhibit motility but not actin-activated MgATP hydrolysis, and dissociate a subset of the calmodulin light chains from the complex. Motility can be restored by readdition of calmodulin. The rate of motility is dependent upon temperature but independent of actin filament length, amount of bound 110K/calmodulin, or ionic strength. Velocity is constant for up to 2h in the assay at 25°C. Tropomyosin completely inhibits the motility of the complex, probably due to drastically reduced actin binding. These results suggest that vertebrate myosins I and II share a molecular mechanism of motility but are uniquely regulated by calcium and tropomyosin.

Tu-PM-E7

KINETIC ANALYSIS OF DICTYOSTELIUM MYOSIN ASSEMBLY R.K. Mahajan and J.D. Pardee. Dept. of Cell Biology and Anatomy,

Cornell University Medical College, New York, NY, 10021. To understand the regulation of *Dictyostelium* myosin II thick filament formation, we have analysed the kinetics of the assembly process. The dependence of assembly rate on myosin concentrations between $2 \times 10^{-8}\text{M}$ and $1.5 \times 10^{-6}\text{M}$ indicates 2nd order kinetics for the overall assembly reaction. As evidenced by stopped-flow rapid dilution assays monitored by light scattering, myosin II assembles with biphasic kinetics consisting of an initial lag phase followed by rapid assembly. Myosin at $2.2 \times 10^{-7}\text{M}$ assembled with an overall reaction half-time of 180s in 50mM K^+ , 1mM Mg^{2+} at pH 6.8. However, assembly kinetics were highly sensitive to buffer conditions. Increased KCl concentrations inhibited the rapid assembly phase of the reaction, but did not affect lag phase kinetics. 10mM Mg^{2+} stimulated both phases. Kinetics were characteristic of polymerization reactions that proceed by a slow nucleation step followed by rapid growth off nuclei. Comparative studies on assembly of skeletal muscle myosin in identical buffers revealed similar biphasic kinetics. EM studies on *Dictyostelium* myosin showed the presence of monomers in high salt before assembly and mixtures of monomers, parallel dimers, and anti-parallel tetramers during lag phase. Subsequent time points indicated growth of filaments by thickening, rather than elongation of nuclei. Combined kinetic and structural data are consistent with a model in which rapid dimerization precedes rate-limiting formation of anti-parallel tetramers, leading to fast lateral addition of myosin to anti-parallel nuclei.

Supported by NIH Grant GM 32458 to J.D.P.

Tu-PM-E6

ACANTHAMOEBA MYOSIN-II MINIFILAMENTS ASSEMBLE IN MILLISECONDS WITH RATE CONSTANTS LARGER THAN EXPECTED FOR A DIFFUSION LIMITED REACTION John H. Sinard and Thomas D. Pollard, Dept. of Cell Biology, Johns Hopkins Medical School, Baltimore, MD 21205

Myosin-II polymerizes by 3 dimerization steps, proceeding from monomers to antiparallel dimers to antiparallel tetramers to octameric minifilaments (Sinard et al (1989) J. Cell Biol. 109: 1537-1548). We have investigated the kinetics of these reactions, initiating assembly by the rapid dilution of salt from 300 to 100 mM KCl in a stopped-flow light scattering apparatus. The reaction is largely completed within 50 ms. Over a 6 fold range of myosin concentrations the time courses can be fit by the successive dimerization mechanism with a single set of rate constants. Other assembly mechanisms do not fit all of the available data. Second order rate constants for the first 2 dimerization steps exceed $10^8 \text{M}^{-1}\text{s}^{-1}$, and derived K_d 's are consistent with equilibrium data. Facilitated diffusion of weakly associated complexes may account for the rapid association reactions. Filament disassembly in 300 mM KCl is even faster than assembly due to larger dissociation rate constants and smaller association rate constants in high than low salt. Aggregation of minifilaments induced by Mg^{++} is much slower and takes many minutes to reach equilibrium.

Tu-PM-E8

HEAVY CHAIN PHOSPHORYLATION AFFECTS MYOSIN FLEXIBILITY IN BIPOLAR FILAMENTS. M.R. Riehm, D.C. Rau, V. Sathyamoorthy and E.D. Korn (Intro. by Hideo Kon) NIDDK and NHLBI, NIH Bethesda, MD 20892.

Phosphorylation of the C-terminal control region of *Acanthamoeba* myosin II, which overlaps the hinge at the HMM-LMM boundary of adjacent monomers in bipolar filaments, inhibits actin-dependent Mg-ATPase activity. Using electric birefringence we observed a negative, slowly relaxing signal corresponding to overall rotation of the bipolar filament, and a fast, positive signal whose intensity indicates the degree of flexing of the HMM arms. When titrating with Mg^{2+} , a steady progression from tetramer to a limiting 16mer was observed along with a logarithmic decrease in the intensity of the fast component. This suggests that the HMM arms are perturbed at a spring of finite flexibility. A stochastic, kinetic model allowed us to estimate the spring force constant, which decrease by a factor of three in phosphorylated myosin filaments. We also inferred that, relative to the dephosphorylated samples, the HMM arms of phosphorylated myosin are more closely aligned to the axis of the bipolar filament.

Tu-PM-E9

LENGTH DEPENDENCE OF ACTIN POLYMERIZATION RATE CONSTANTS

Chris M. Coppin* and Paul C. Leavis*, *Tufts Univ. Sch. of Med. Dept. of Physiology and *Boston Biomed. Res. Inst., Boston Ma.

The rate constants determining the subunit flux at the end of an actin filament are generally considered to be independent of the length of the filament. We used the nucleating and barbed-end capping protein human plasma gelsolin to control the number (and therefore the length) of growing pyrene-labeled actin filaments. By measuring the rate of polymerization of the actin in the presence of human plasma gelsolin, we have shown that the association and dissociation rate constants at the pointed end are strongly dependent on the length of the filament at all temperatures except at a unique temperature that nearly coincides with human body temperature. We speculate that the temperature at which the length-dependence of the rate constants vanishes may be determined by the binding of various actin-binding proteins (like gelsolin) many subunits away from the pointed end. A length dependence of the rate constants could serve as a means of modulating the actin filament length distribution *in vivo*.

Tu-PM-E11

Functional and Structural Domains of a 120,000 Dalton Actin Binding Protein from Dictyostelium discoideum. A.R. Bresnick, Albert Einstein College of Medicine, Bronx, NY.

Tryptic digestion of ABP-120 (Condeelis et al. JCB 99:119s, 1984) generates a ladder of peptides differing in molecular weight by 10,000 daltons, indicating a structural repeat within the molecule. A number of peptides bind actin with the smallest having a molecular weight of 17,000 daltons (T17). Our sedimentation assays also show that a peptide of 14,000 daltons (T14) does not bind actin. Using the full length cDNA sequence (Noegel et al. JCB 109:607, 1989) and protein sequencing techniques, we have determined that T17 begins at residue 89 while T14 begins at residue 116. Therefore we have localized a domain of ABP-120 that is essential for actin binding activity. This domain is at the end of the molecule, distal from the repetitive β -sheet region predicted from the cDNA sequence. Tryptic digestion rapidly generates a 89,000 dalton tail and a 31,000 dalton head which begins at residue 89. This head contains the actin binding domain and is predicted to contain one of six structural repeats. Longer digestion times indicate that the tail, consisting of five structural repeats, is protease-resistant. These results and rotary shadowing (Condeelis et al., 1984) predict an anti-parallel dimer in which the monomers are offset by 41,000 daltons at the N-terminus. Supported by T32 CA09475 and grants from NIHGMs.

Tu-PM-E10

ACTIVE AND INACTIVE FORMS OF TENSIN, AN ADHESION PLAQUE PROTEIN WHICH CAPS THE BARBED ENDS OF ACTIN FILAMENTS. James A. Butler and Shin Lin. Dept. of Biophysics, Johns Hopkins Univ., Baltimore MD 21218.

Tensin, a 150 kD vinculin-binding protein purified from chicken gizzard, has been immunolocalized at adhesion plaques of fibroblasts (Risinger & Lin, *J. Cell Biol.* 107: 256a, 1988). The protein can be separated by isoelectric focussing into two major forms with pI between 7 to 8.5. The more basic form is highly effective in inhibiting monomer association and dissociation from the barbed end of F-actin and co-sediments with the filaments. In contrast, the more acidic form does not interact with F-actin by these criteria. The two forms have similar peptide maps, but chromatography on a Sephacryl S300 column showed that the active form has a larger Stokes radius (79 Å vs 68 Å). While the basis for the difference in activity between the two forms remains to be determined, this study suggests that tensin-related isoforms may play a regulatory role in assembly and membrane-association of actin filaments in muscle and nonmuscle cells. (Supported by NIH grant GM22289 and an AHA grant-in-aid).

Tu-PM-E12

Studying the Large-Scale Structure of Actin/Filamin Mixtures by Tracer Diffusion and Optical Microscopy L. Hou, K. Luby-Phelps, and F. Lanni. Center for Fluorescence Research in Biomedical Sciences, and Department of Biological Sciences, Carnegie Mellon University, Pittsburgh, PA 15213.

Diffusion of size-fractionated fluorescent Ficoll tracers in mixtures of filamin and F-actin was measured by fluorescence recovery after photobleaching (FRAP). In solutions of F-actin with no filamin, the relative diffusion coefficient of the tracer (D/D_0), decreased with the tracer radius (R_T) and with the actin concentration. In matrix of actin co-polymerized with filamin, D/D_0 increased weakly with filamin-to-actin molar ratio (F:A). DIC and phase contrast microscopy suggested that the reduction of hindrance was due to the bundling of F-actin filaments which increased the effective void volume fraction of the matrix. Three dimensional arrays of highly-interconnected bundles of F-actin become visible when F:A exceeded 1:140 in a range of actin concentrations from 0.1 to 9 mg/ml. To observe bundle formation, a dialysis optical cell was constructed so that actin polymerization could be induced with virtually no shear flow. Spontaneous F-actin bundling was observed in ≤ 2 min after initiating polymerization in a 1mg/ml actin-filamin mixture, resulting in a stable three dimensional structure in about 3 min. By studying the mobility of monodisperse latex particles 0.05 to 0.7 μ m in diameter, we also demonstrated that pure F-actin solutions exhibit a percolation cutoff. The mobile-to-immobile transition was found to be a sharp function of F-actin concentration. We interpret our results in terms of the structure of the cytoskeleton and the transport of macromolecules and organelles in it. Supported by NIH GM 34639, NSF 86-16089 and NIH AR32461 (to D. L. Taylor).

Tu-PM-E13

THE STRUCTURE OF AN IN VIVO ACTIN GEL. D.J. DeRosier* and L.G. Tilney.* *Rosenstiel Center, Brandeis University, Waltham, MA 02254 and †Department of Biology, University of Pennsylvania, Philadelphia, PA 19104.

The erect array of stereocilia on each hair cell of the inner ear transduces fluid motions into voltage changes. The cytoskeleton responsible for the erect stereocilia contains three kinds of f-actin assemblies: bundles, which fill the core of the stereocilia; ribbons, which extend as rootlets from the bundles into the body of the cell; and, of especial interest, a gel which, by engulfing the rootlets, holds the stereocilia erect. The gel comprises thousands of bewhiskered actin filaments which look and behave like flexible test tube brushes having 65 nm long bristles. Such a simple analogue embodied in a Monte Carlo computer program, accurately simulates electron micrographs and quantitatively accounts for the distribution of filaments in the gel. Unlike the perfectly aligned filaments in a bundle or ribbon, the bewhiskered filaments in the gel can take up any orientation and will fill every available space as long as no two filaments are less than 65 nm apart.

Tu-PM-E14

DYNAMICS OF THE ACTIN-BASED CYTOSKELETON OF SERUM-DEPRIVED AND GROWTH-FACTOR-STIMULATED FIBROBLASTS. K.A. Giuliano and D.L. Taylor, Department of Biological Sciences and Center for Fluorescence Research in Biomedical Sciences, Carnegie Mellon University, 4400 Fifth Avenue, Pittsburgh, PA 15213.

Fluorescent analogs of actin and conventional myosin (myosin II) were injected into serum-deprived Swiss 3T3 fibroblasts. Using multi-mode time-lapse microscopy we found that fibers containing both actin and myosin II continuously peeled off from the cytoplasm-membrane interface and were transported at an average rate of 16 $\mu\text{m}/\text{h}$ toward the nucleus where they dissappeared. Treatment of these cells with either 10% serum or 10 nM thrombin often caused an immediate cytoskeletal reorganization followed by a contraction of the fibers (L_i/h of approximately 10). We are using a variety of inhibitors and new fluorescent analogs to define the molecular basis of fiber formation, transport, and contraction. Supported by NIH Program Project GM34639.

Tu-PM-F1

Molecular Genetic Studies of Visual Pigments. Jeremy Nathans, Howard Hughes Medical Institute, Johns Hopkins University Baltimore, MD 21205

We have taken two genetic approaches to the study of visual pigments. To study the role of single amino acids and protein domains in visual pigment structure and function we have constructed and expressed site directed mutants of bovine rhodopsin. One series of mutants tests the role of charged amino acids in the putative transmembrane segments on the spectral properties of rhodopsin. There is surprisingly little effect of mutation at the six candidate residues. A second series of mutants tests the effect of changing each glutamate and aspartate to a neutral residue. A second approach involves identifying and analyzing inherited alterations in human visual pigments using a combination of psychophysical and molecular genetic methods. Because visual pigment mutations have little effect on viability or fecundity, these alleles should persist in the population.

Tu-PM-F3

NOVEL PROTEINS MOLECULES MAY MEDIATE ODORANT DETECTION Randall R. Reed, David T. Jones and Heather A. Bakalyar Dept of Molecular Biology and Genetics, Johns Hopkins School of Medicine, Balt. MD 21205 Previous biochemical studies have demonstrated that certain odorants stimulate a GTP-dependent increase of cAMP levels in olfactory neuronal cilia. Our laboratory has identified a novel G_{sa} subunit termed " $G_{olf\alpha}$ " expressed exclusively in olfactory sensory neurons (*Science* **244**, 790-795). Recently, we have cloned a bovine brain adenylyl cyclase (type I, *Science* **244**, 1558-1564). Low stringency hybridization of a rat olfactory cDNA library with the type I clone revealed a distinct form of cyclase, adenylyl cyclase type III. The two cyclases share considerable amino acid similarity and each has a primary protein sequence which predicts 12 membrane spanning domains. The role of the membrane span in protein function remains to be determined. Northern analysis indicates that type III mRNA is confined to the primary sensory neurons of the olfactory epithelium. Thus, like G_{olf} , this olfactory specific adenylyl cyclase appears to be a component in a signal transducing cascade specialized for odorant detection.

Tu-PM-F2**REGULATION OF G-PROTEIN COUPLED RECEPTORS.**

Jeffrey L. Benovic, Marc G. Caron and Robert J. Lefkowitz, Fels Institute for Cancer Research and Molecular Biology, Philadelphia, PA and Duke University Medical Center, Durham, NC.

The regulation of cellular sensitivity, often termed desensitization, is observed in diverse biological systems. In many of these systems a stimulus dependent phosphorylation of cell surface receptors appears to play a key role in the desensitization process. The β -adrenergic receptor-coupled adenylyl cyclase system has proven to be an excellent model for studying desensitization. Rapid agonist-specific or homologous desensitization of this system appears to be largely mediated by phosphorylation of the receptor by a specific kinase, termed the β -adrenergic receptor kinase (β ARK). The primary structure of β ARK has been elucidated by screening a bovine brain cDNA library with oligonucleotides derived from partial amino acid sequence. The β ARK cDNA codes for a protein of 689 amino acids (79.7 kD) with a catalytic domain most similar to protein kinase C and the cAMP dependent protein kinase. When expressed in COS-7 cells the kinase specifically phosphorylates the agonist-occupied form of the β -adrenergic receptor. A cDNA similar to β ARK has also been isolated by low stringency hybridization. This cDNA encodes a protein of 688 amino acids (79.7 kD) with 85% amino acid identity with β ARK. These results suggest that β ARK is a member of a multigene family of receptor kinases which function to regulate cellular sensitivity to environmental stimuli.

Tu-PM-F4**RECEPTOR/G-PROTEIN SIGNALING SYSTEMS CONTROL *DICTYOSTELIUM* DEVELOPMENT.**

R. Johnson, T.J. Sun, R. Vaughan, M. Caterina, P. Van Haastert, R.E. Gundersen, G.S. Pitt, S.M. Voglemeier, M.B. Pupillo, and P.N. Devreotes. Dept. of Biol. Chem., Johns Hopkins Medical School, Baltimore, MD 21205.

Biochemical evidence for the role of cAMP receptors (cAR's) during development in *Dictyostelium* is well documented. Recently, a family of three cAMP receptor subtypes (cAR1, cAR2, and cAR3) have been cloned and sequenced. Transformed cell lines expressing either cAR1 or cAR3 display high levels of cAMP binding. Photoaffinity labelling with cAMP shows that cAR1 and cAR3 are 40 and 70 kD proteins, respectively. Cell lines which lack cAR1 by antisense mutagenesis are blocked in most aspects of the developmental program. We have previously reported the sequences of two G-protein α subunit cDNAs ($G_{\alpha 1}$ and $G_{\alpha 2}$) from *Dictyostelium*. A third G-protein α subunit, $G_{\alpha 3}$, has recently been cloned. The *fgd A* locus has been shown to be the $G_{\alpha 2}$ gene since its alleles contain either deletion or point mutations in the $G_{\alpha 2}$ gene. Upon cAMP stimulation, $G_{\alpha 2}$ undergoes a time dependent transition in electrophoretic mobility from 40 to 43 kD due to phosphorylation on serine residue(s). These modifications are rapid and transient and coincide with the time course of cAMP activated physiological responses.

Tu-PM-F5

VISUAL TRANSDUCTION IN PLANT CELLS: OPTICAL RECORDING OF RHODOPSIN-REGULATED INTRACELLULAR PROCESSES FROM *CHLAMYDOMONAS*. P. Hegemann and R. Uhl, MPI für Biochemie, 8033 Martinsried,

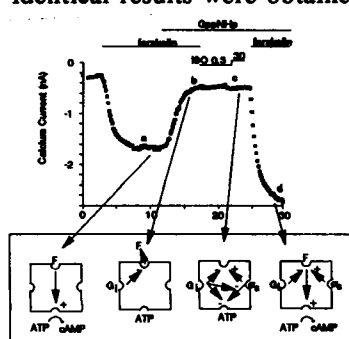
Visual transduction in the unicellular alga *Chlamydomonas* has been studied using flash-induced light scattering signals reflecting structural changes as a consequence of photon absorption and membrane depolarisation. Flash-induced optical signals from *Chlamydomonas* are fast, repeatable, graded with flash energy and adaptive. Their time course correlates with flash-induced movement re-sponses, and the responsible visual pigment can be shown to be a rhodopsin. The optical technique is sensitive enough to pick up single quantum responses, establishing that *Chlamydomonas* cells are quantum detectors. Thus light scattering studies, which have greatly aided the understanding of rapid processes in visual transduction of higher animals, may also prove to be a powerful and non-invasive tool for the in vivo examination of molecular processes in the phototaxis of unicellular microbes.

Tu-PM-F7

G-PROTEINS, G_s AND G_i , ACT AT SEPARATE SITES ON ADENYLYL CYCLASE TO REGULATE VOLTAGE-GATED Ca^{2+} -CURRENTS IN CARDIOMYOCYTES. R.E. White*, A. Lagrutta, T.D. Parsons, H.C. Hartzell. Emory University, Atlanta, GA 30322, *NIEHS, Res Tri Park, NC 27709

Internal perfusion of isolated cardiomyocytes with the non-hydrolyzable GTP analog, GppNHp (GN) rapidly reduced the forskolin (FORSK) stimulated voltage-gated Ca^{2+} -current (I_{Ca}). GN (30-500 μ M) decreased the 3 μ M FORSK I_{Ca} by $74 \pm 17\%$ ($n=32$). The decrease in FORSK I_{Ca} was due to a 50-fold increase in the EC_{50} for stimulation with FORSK, without any change in efficacy; and was blocked by the addition of a 10-fold excess of GTP to the internal solution. Subsequent application of isoproterenol produced no response, but surprisingly, re-exposure to FORSK resulted in an increase in I_{Ca} that was similar to the initial FORSK response (see fig). Virtually identical results were obtained in 18 cells. This

demonstrates that although G_s activation had no effect on adenylyl cyclase's (AC) catalytic activity, it did alter the affinity of AC for FORSK. This suggests that the activated subunits of both G_s and G_i were simultaneously bound to AC. (NIH HL21195 to HCH)



Tu-PM-F6

EOSINOPHIL SECRETION OCCURS THROUGH EXOCYTOSIS MEDIATED BY A G PROTEIN

M. Lindau¹, O. Nüsse¹, O. Cromwell², A. B. Kay² & B. D. Gomperts³
¹Biophysics Group, Free Univ. Berlin, D-1000 Berlin 33, FRG.
²Dept. Allergy & Clin. Immunol., National Heart & Lung Inst. London, UK.
³Dept. Physiol., Univ. College London, UK.

Eosinophils have been of great clinical interest but very little is known about the secretory mechanism in this cell type. Using time-resolved patch-clamp capacitance measurements we demonstrate that secretion is accomplished by exocytosis involving sequential fusion of single granules with the plasma membrane. The fine structure of the capacitance change suggests fusion of two classes of granules. Patch-clamp and permeabilisation experiments show that exocytosis is stimulated by intracellular application of GTP γ S. In the presence of ATP elevated $[Ca^{2+}]_i$ is not required but $[Ca^{2+}]_i$ modulates exocytosis. Fura-2 fluorescence measurements in the whole-cell patch-clamp configuration show that GTP γ S also generates Ca transients preceding the main phase of granule fusion.

Supported by DFG Sfb 312 / B6

Tu-PM-F8

ANTIBODIES TO PTX-SENSITIVE G PROTEIN α -SUBUNITS BLOCK THE ACTIVATION OF MUSCARINIC ATRIAL K^+ CHANNEL CURRENTS. A. Yatani, K. Okabe, A.M. Spiegel*, L. Birnbaumer** and A.M. Brown. Departments Molecular Physiology & Biophysics and Cell Biology**, Baylor College of Medicine, Houston, TX 77030 and National Institute of Health*. The monoclonal antibody 4A raised against the α -subunit of frog transducin immuno-reacts with α_{1-3} and blocks muscarinic activation of atrial K^+ channel currents ($K^+[ACh]$). To further examine the functional interactions of G protein α -subunits with receptors and effectors in native membranes, we tested antibodies (Ab's) raised against synthetic decapeptides corresponding to the C-termini of four different G protein α -subunits, α_{1-3} , (Ab EC), α_{1-1} and α_{1-2} (Ab AS), α_{1-3} (Ab GO) and α_{1-3} (Ab RM) on $K^+[ACh]$ using I-O patch recordings from adult guinea pig atrial cells. $K^+[ACh]$ were activated by carbachol at 10 μ M in the presence of 100 μ M GTP. Ab EC at 10 nM ($IC_{50}=5$ nM) completely blocked $K^+[ACh]$, while Ab AS required 5-10 times higher concentrations ($IC_{50}=20$ nM). Ab GO had small blocking effect at concentrations higher than 10 nM, whereas Ab RM had no effect. Control rabbit immunoglobulin (IgG) was also ineffective. Block was due to a decrease in the probability of channel opening; neither open time nor unit conductance were changed. Block was reversed by subsequent addition of GTP γ S (100 μ M) or preactivated α_{1-3} at 10 pM after washing out the Ab's. The data suggest that α_{1-3} is preferred in the mediation of muscarinic activation of $K^+[ACh]$.

Tu-PM-G1**HEADGROUP CONFORMATION OF A LIQUID CRYSTALLINE PHOSPHATIDYLCHOLINE BILAYER.**

Michael C. Wiener and Stephen H. White. *Department of Physiology and Biophysics, University of California at Irvine, Irvine, CA 92717.* The structure of L_α DOPC at 66% RH (5.4 waters/lipid) has been determined by quasi-molecular modeling and a joint refinement procedure utilizing x-ray and neutron diffraction data. The distributions of the phosphocholine group in the x-ray and neutron scattering density profiles differ significantly, enabling the phosphate and choline distributions to be separated by a simple center-of-scattering formalism. A comparison of the widths of the distributions to their molecular radii, through a Debye-Waller/convolution analysis, provides estimates of the ranges of molecular motion of these groups. The choline, much more mobile than the phosphate, has a significant probability of venturing into the hydrophobic region of the bilayer. Steric hindrance of the headgroups of apposed bilayers is clearly shown. We believe that the real-space distributions of phosphate and choline obtained are the first direct determination of detailed headgroup conformation in a fluid bilayer. Supported by NIH and NSF.

Tu-PM-G3

PARTITIONING AND MEMBRANE DISORDERING EFFECTS OF n-ALKANOLS IN PHASE SEPARATED MIXTURES OF PHOSPHATIDYLCHOLINES. Martha Sarasua, Susan Dakin, and Allan Atienza; *Department of Surgery, Cleveland Metropolitan General Hospital and Case Western Reserve University, Cleveland, Ohio.*

The partitioning and membrane disordering effects of n-alkanols in phase separated mixtures of phosphatidylcholines (PCs) (PC_{12}/PC_{16} and PC_{14}/PC_{18} ; numbers indicate fatty acid chain length) were characterized as a function of temperature. Partitioning of ^{14}C -alcohols into these PC mixtures and their effects on the fluorescence polarization of diphenylhexatriene (DPH) were measured. Differential Scanning Calorimetry (DSC) scans verified the presence of phase separation in the mixtures. The alcohols selectively partition into the lower chain length PC in the mixtures. Alcohol effects on DPH polarization were maximal at the main phase transitions in each mixture and were comparable in magnitude to the effects observed in pure PCs.

Tu-PM-G2**MOLECULAR SPRING MODEL FOR 22:6w3 FUNCTION IN MEMBRANES**

Holte, L.L.*[†], Deese, A.J., Ryba, N.[†], Watts, A.[†], and Dratz, E.A.*[†]

*Montana State Univ., Bozeman, MT; [†]Oxford Univ., Oxford, UK

Docosahexaenoic acid (22:6w3) has an essential role in the function of photoreceptors and synaptic endings but the molecular mechanism is unknown. Low angle x-ray and neutron diffraction indicates that 22:6 fatty acids lead to thin (ca 27Å) hydrocarbon layers in bilayers. We support this conclusion with deuterium NMR studies of phospholipid bilayers. Conformational energy calculations imply that the most stable conformation of the 22:6 chain are short, squat helices.

Phospholipids containing 22:6, reconstituted with rhodopsin, are easily damaged by oxygen. Phospholipids were purified by preparative HPLC and the products characterized by Flow FAB mass spectrometry. Light stimulated rhodopsin forms metarhodopsin II (MII) which excites the cell. Evidence will be presented that the 22:6 chain conformation is coupled to and facilitates the MII conformational change by acting as a "molecular spring" accommodating the planar expansion of MII rhodopsin by forming a conformation with less planar area. Supported by NIH/EY06913

Tu-PM-G4

MONTE CARLO STUDIES OF INTERACTIONS IN MODEL MEMBRANES: GRAMICIDIN A AND CHOLESTEROL. J. Xing and H.L. Scott, *Department of Physics, Oklahoma State University, Stillwater, Ok. 74078.*

The Monte Carlo method has been used to examine the equilibrium properties of lipid chains in a model membrane interacting with either cholesterol or gramicidin A. The gramicidin A-lipid simulation consists of 94 lipid chains and one gramicidin A monomer (co-ordinates generously supplied by E. Jakobsson) in a lamellar array. Three sets of cholesterol-lipid simulations were carried out with 3, 7, or 13 cholesterol molecules and 97, 93, or 87 lipid chains, respectively, in the lamellar array. In all cases the Monte Carlo algorithm used is identical to one used earlier (Scott and Kalaskar, *Biochemistry* 28, 3687-3691). The main results of the simulations consist of average order parameter profiles for chains which are near neighbors to the cholesterol molecules or to the gramicidin A monomer, and similar profiles for the remaining (bulk) chains. In addition, snapshots of single configurations are obtained for graphic display. The simulations indicate that a single gramicidin A monomer or isolated cholesterol molecules do not affect the chain order parameter profiles, although some hindrance of rotational mobility may be inferred from the rejection rates. At a high cholesterol concentration significant differences appear in the order parameter profiles for those chains which are near neighbors to two cholesterol, compared to the bulk chains.

Tu-PM-G5

COHESIVE PROPERTIES (ELASTIC DEFORMATION AND FAILURE) OF LIPID BILAYERS CONTAINING CHOLESTEROL. D. Needham and R. S. Nunn, Mechanical Engineering and Materials Science, Duke University, Durham, N.C. 27706. Giant bilayer vesicles were reconstituted from several lipid and lipid/cholesterol(CHOL) mixtures: Stearoyllecithin phosphatidylcholine (SOPC), Diarachidonyl phosphatidylcholine (DAPC), SOPC:CHOL, Bovine Sphingomyelin (BSM):CHOL, DAPC:CHOL and extracted red blood cell(RBC) lipids. Single walled vesicles were manipulated by micropipet suction and the following membrane material properties were determined; elastic area compressibility modulus, critical areal strain, tensile strength, and failure energy. The elastic area compressibility moduli for these bilayers ranged from 57 dyn/cm for DAPC to 1734 dyn/cm for BSM:CHOL. For the SOPC:CHOL system the change in elastic modulus was modelled by a property averaging composite theory involving two bilayer components, a lipid:cholesterol:1:1.35 complex and uncomplexed lipid. Bilayer toughness showed a maximum value at ~40 mol%CHOL and its form was correlated with a minimum in the free energy of mixing the two bilayer components. These breakdown energies are only a fraction of kT indicating that many molecules may be involved in forming the defect structure that leads to failure.

Tu-PM-G7

THE FUSION SITE OF INFLUENZA HA-EXPRESSING FIBROBLASTS REQUIRES MORE THAN ONE HA TRIMER. H. Ellens¹, J. Bentz², D. Mason³ and J.M. White³. ¹Drug Delivery Dept. Smith, Kline and French Labs, King of Prussia, PA 19406, ²Dept. Biosci. & Biotechn., Drexel Univ. Philadelphia, PA 19401. ³Dept. of Pharmacol., Univ. of California, San Francisco, CA 94143.

To learn how many hemagglutinin (HA) trimers are necessary for membrane fusion, we used two NIH 3T3 fibroblast cell lines, expressing HA at different densities. The HAb-2 cells show a 1.9 fold higher level per mg protein than the GP4F cells, hence we argue a 1.9 fold higher HA surface density. A competition experiment with toxin-containing and empty liposomes allows us to quantitate the number of liposomes fusing per cell. The HAb-2 cells fuse with 1 in every 75 and the GP4F cells with 1 in every 330 bound liposomes. Hence, the HAb-2 cells, with 1.9 times the surface density of HA, show 4.5 times more fusion per bound liposome. We conclude: (i) One HA molecule is not sufficient to induce fusion. (ii) The HA bound to glycoporphin cannot be the HA which induces fusion. A molecular model of this fusion event is presented, which explains why more than one HA is required for fusion and which also describes the flow of lipids from physico-chemical principles.

Tu-PM-G6

MODULATION OF POLY(ETHYLENE GLYCOL)-INDUCED FUSION BY MEMBRANE HYDRATION.

Stephen W. Burgess¹, Thomas J. McIntosh², & Barry R. Lentz¹. ¹Biochemistry Dept., University of North Carolina, Chapel Hill, NC 27599, and ²Duke University, NC 27710. Intro. by Walter A. Shaw.

Large, unilamellar vesicles were prepared by the extrusion technique. Vesicles were composed of either dioleoyl phosphatidylcholine (DOPC) with 0.5 mol% monooleoyl phosphatidylcholine (lysoPC) or various molar ratios of DOPC and dilauroyl phosphatidylethanolamine (DLPE). Fusion was revealed via the ANTS/DPX assay for contents mixing and leakage, the DPHpPC lipid probe for membrane mixing, and quasielastic light scattering for vesicle size growth. As membrane hydration decreased, the concentration of poly(ethylene glycol) (PEG) required to induce fusion also decreased. Vesicles containing DOPC/lysoPC fused at 35wt% PEG while vesicles containing DLPE/DOPC (85:15) fused at 20wt% PEG. An intermediate ratio of PE/PC (65:35) fused at 25 wt% PEG. From differential scanning calorimetry of PE/PC unilamellar vesicles in PEG, we concluded that PEG did not induce a hexagonal phase transition or PE/PC phase separation. X-ray diffraction studies of multi- and unilamellar vesicles indicated that the fluid layer between vesicles was 5-7Å at PEG concentrations where vesicles were first induced to fuse. These results indicate that a requirement for the fusion process is reducing the inter-bilayer water layer to 2-3 water molecules. This intimate bilayer juxtaposition is necessary but apparently not sufficient to induce the fusion event. Supported by USPHS Grant GM32707 to BRL.

Tu-PM-G8

A HIGH-SENSITIVITY DIFFERENTIAL SCANNING CALORIMETRIC STUDY OF THE INTERACTION OF MELITTIN WITH DIPALMITOYLPHOSPHATIDYLCHOLINE FUSED UNILAMELLAR VESICLES

T.D. Bradrick¹, E. Freire², and S. Georghiou¹
¹Physics Dept., Univ. of Tenn., Knoxville, TN and ²Biology Dept., Johns Hopkins Univ., Baltimore, MD

We have used high-sensitivity DSC to examine the interaction of monomeric and tetrameric melittin in solution with DPPC FUVs. A broad range of lipid-to-protein molar ratios was used to explore the effects of these two protein species on the lipid thermotropism. From our results we have obtained information regarding the state of aggregation of melittin in lipid bilayers. We find the protein binds to lipid bilayers as an aggregate when it is tetrameric in solution, whereas it binds as a monomer when it is monomeric in solution. In the case of monomeric melittin in solution we have also obtained evidence that free melittin in solution plays a role in the mechanism of melittin-induced vesicle fusion, perhaps through the formation of protein bridges between apposed vesicles. (Supported by NIH grants GM32433 to S. G. and GM37911 to E. F.)

Tu-PM-G9

A LIPOSOME-FORMING ARCHAE-BACTERIAL

LIPID by E. L. Chang¹, Alan Rudolph¹, and Shi-Lung Lo^{2*}, ¹Center for Bio/Molecular Science and Engineering, Code 6090, Naval Research Laboratory, Washington, D.C. 20375-5000, and ²Geo-Centers, Newton Upper Falls, MA 02164

*Present address: NEN Products, DuPont, 549 Albany St., Boston, MA 02118

Lipids from the polar lipid E (PLE) fraction of the thermoacidophile *Sulfolobus acidocaldarius* were purified by reverse-phase chromatography, followed by TLC and methanol precipitation. These bipolar tetraether lipids disperse easily in aqueous-media forming micron-sized multilamellar liposomes. Freeze-fracture studies show that the liposomes cross-fracture rather than follow any midplane of a bilayer. This behavior is consistent with results from freeze-fracture of the native membranes of *S.acidocaldarius* which also cross-fracture. Thus, we have demonstrated that purified tetraether lipids can, *per se*, form liposomes without the aid of either monopolar lipids or proteins and that the structure of the membrane is most likely non-bilayer in nature. Physical characterizations show that hydrolyzed tetraether lipids do not form a stable film at the air/water interface while PLE lipids can hold pressure. FTIR results point to a very disordered hydrocarbon environment for the archaebacterial lipids.

Tu-Pos1

BASE STACKING AND UNSTACKING AS DETERMINED FROM A DNA DECAMER CONTAINING A FLUORESCENT BASE

P. G. Wu and T. M. Nordlund, Dept. of Biophysics, University of Rochester, Rochester, NY 14642; B. Gildea and L. W. McLaughlin, Dept of Chemistry, Boston College, Chestnut Hill, MA 02167

Time-resolved fluorescence decays of a single-stranded DNA decamer d(CTGAAT5CAG) at several temperatures are measured and analyzed, where d5 is a fluorescent base 1-(β -D-2'-deoxyribo-5-methyl-2-pyrimidinone. d5 is resolved into fully unstacked, loosely stacked, and stacked states, according to their fluorescence lifetime characteristics and temperature dependence of their associated amplitudes. These states are in slow exchange compared to their fluorescence decay rates. The population of the fully extended and unstacked state is very small and decreases with increasing temperature. The loosely stacked state whose fluorescence can still be efficiently quenched by other DNA bases, occupies a large portion of the conventionally defined unstacked state. The stacking enthalpy and entropy of d5 with thymine or cytosine are calculated to be -6.6 Kcal/mole and -22 cal/mole-K, respectively. This work shows that fluorescent bases in DNA can be used to study the local conformations of bases.

Tu-Pos3

MELTING STUDIES OF RNA PURINE MISMATCHES.

Sarah E. Morse and David E. Draper, Department of Chemistry, Johns Hopkins University, Baltimore, MD 21218

Phylogenetic comparison of rRNA has shown that some non Watson-Crick base juxtapositions are evolutionarily conserved. These may function as protein recognition sites or stabilize tertiary structures. Using solid support oligonucleotide synthesis we have constructed several self-complementary RNAs containing A-A, A-G, and G-G mismatches in a variety of sequence contexts. The helix to coil transition of these oligomers was studied by thermal denaturation. All of the oligomers studied show a two state transition that can be analysed by the method of Turner and Petersheim (*Biochemistry* 22 256-263,1983) to provide the ΔH° , ΔS° and ΔG° of helix formation. Comparison of thermodynamic values for a mismatch to those obtained for a reference helix allows the change in enthalpy, entropy and free energy due to the mismatch to be determined. A G-G mismatch does not perturb ΔH° but does increase ΔS° , destabilizing ΔG° at 37°C by 4.2 kcal/mole. In contrast an A-G mismatch results in a less favorable ΔH° and ΔS° but the change in ΔG° at 37°C is only 2.5 kcal/mole. The effects of ionic strength, pH and Mg ion concentration on mismatch stability are being measured.

Tu-Pos2

EFFECTS OF FINITE LENGTH DNA ON THE HELIX-COIL TRANSITION. Marcia O. Fenley, Gerald S. Manning and Wilma K. Olson, Department of Chemistry, Rutgers University, New Brunswick, NJ 08903

We make an analysis of the chain length dependence of thermodynamic properties associated with the helix-coil transition in DNA. Calculations of the counterion binding fraction (of coiled and helical forms of DNA) and the DNA melting temperature are performed over a broad range of monovalent and divalent salt concentration. These calculations were done within the counterion condensation theory framework, based on both the linear and three-dimensional spatial phosphate charge distribution of DNA. For the coil form in the latter model, the distribution of phosphate distances is found from Monte Carlo sampling studies. (Supported by USPHS grants GM36284 and GM34809).

Tu-Pos4

FORMATION AND LOSS OF DNA CROSSLINKS

INDUCED BY MELPHALAN AND NITROGEN MUSTARD. Christian G. Reinhardt, Richard A. Grucza, Margaret I. Kaminsky and Joanne Yeh, Dept. of Chemistry, Rochester Inst. Technology, Rochester, New York 14623

The formation and loss of nitrogen mustard (HN2) and melphalan (PAM)-induced DNA inter strand X-links have been characterized in solution by spectrophotometric methods, and compared to the in-vivo differences in rates of formation and repair of X-links induced by these clinically important anti cancer drugs. Our solution kinetic studies support the following interpretations: (1) the protracted induction of DNA-PAM X-links in-vivo in comparison to HN2 is primarily due to a slower DNA alkylation rate; (2) the accelerated rate of removal of HN2-DNA X-links in-vivo does not appear to be due to enzymatic repair of the induced lesion, but instead due to an increased rate of depurination at the HN2-DNA X-link site. The solution kinetic data on the steady-state and intrinsic rates of formation and loss of DNA X-links induced by HN2 and PAM will be presented. Some implications of these measurements for interpreting the differences in cytotoxic effects and pharmacokinetic behavior of these drugs will be discussed. Supported by CA47734-01 from NIH.

Tu-Pos5

INTERACTIONS OF SELECTED ANILINO-ACRIDINE ANALOGS WITH DNA: CORRELATION OF THE CONFORMATIONAL DYNAMICS AND THERMODYNAMIC PROPERTIES

Randy M. Wadkins and David E. Graves,
Department of Chemistry, University of Mississippi, University, Mississippi 38677

Thermodynamic profiles of a series of anilino-acridine analogs binding to native and synthetic DNAs were determined. These studies examined the effects of substituent type and position (on the aniline ring) with respect to the thermodynamic properties associated with DNA complex formation. Distinct differences in the binding profiles were observed for these structurally similar analogs. To determine the role that substituent modification and/or position plays in influencing the binding of these analogs to DNA, conformational dynamics were performed using molecular mechanical and semi-empirical modeling techniques. From these studies, information concerning the structural orientation of the 9-anilino groups with respect to the acridine chromophore is obtained which provides insight into the molecular geometry of the drug-DNA complex.

Tu-Pos7

THE ASSOCIATION OF ETHIDIUM AND PROPIDIUM TO DNA OLIGOMERS WITH ONE BINDING SITE.

Luis A. Marky, Department of Chemistry, New York University, New York, NY 10003.

The intercalative binding of drugs to nucleic acid duplexes have been studied extensively by a wide range of experimental techniques. X-ray structural studies of drug-DNA complexes have revealed that intercalators bind to DNA duplexes with a sequence preference for a 5'-pyr-pur-3' site, with an exclusion of at least two base pairs. In solution the binding of ethidium and propidium follow the above rules, but positive cooperativity has been observed with some polymer sequences. To eliminate the effects of site-site interactions, the association of ethidium and propidium to DNA molecules containing one binding site was studied. A combination of titration calorimetry and UV-VIS spectroscopy techniques was employed to measure directly binding enthalpies and association constants, as well as complex stoichiometry as a function of temperature and ionic strength. Complete thermodynamic profiles will be reported and correlated with available structural information. This work was supported by Grants GM42223 and BRSG SO7 RR 07062 from the National Institute of Health.

Tu-Pos6

CALCULATIONS OF THE IONIC DISTRIBUTION AROUND DNA. A.E. Kister and A.A. Rashin.
Dept. Physiology and Biophysics, Mount Sinai School of Medicine, New York, NY10029

The method based on the Boundary Element technique is used to compute ionic atmosphere around DNA-s modelled as cylinders with helical distributions of charges. The evaluation of contributions of different factors into the stabilization of alternative forms of DNA is performed. Among such factors are: interactions of phosphates with water, and with ionic cloud; contributions of "images" and correlations. Calculations based on the solution of the non-linear Poisson-Boltzmann equation demonstrate that the ~ 10 fold calculated variation in the ionic density around DNA is a significant factor in the stabilization of different forms of DNA. "Images" are found to contribute $\sim 10\%$ of the total polarization effects. The method allows Monte-Carlo or Molecular Dynamics studies of the ionic distribution around DNA. Such studies lead to the estimates of the correlation effects in the ionic atmosphere.

Tu-Pos8

LIGHT SCATTERING OF MONONUCLEOSOMAL DNA: IONIC STRENGTH, VALENCE, AND DNA CONCENTRATION DEPENDENCE. Marilyn E. Ferrari and V. A. Bloomfield, Dept of Biochemistry, University of Minnesota, St. Paul, Minnesota 55108.

The slow-fast transition in polyelectrolytes is characterized by a large decrease in M_{app} and two diffusion coefficients (D) whose ratio is as large as 100. The fast mode is consistent with theoretical predictions; the slow mode may reflect collective motions. We have undertaken a thorough investigation of salt and polymer concentration effects, using 150 bp mononucleosomal DNA whose rigidity avoids complications from changes in polymer conformation. DNA concentrations ranging from 0.5 - 18 mg/ml enable extension of the transition into the semidilute regime. We observe the following diffusion behavior when the NaCl concentration is varied from 0.1mM - 1.0 M. 1) The slow mode appears at a higher salt concentration as the DNA concentration is increased. 2) D_{app} for the slow mode shows little salt or DNA concentration dependence. 3) The contribution of the slow mode to the diffusion process shows little dependence on DNA concentration for $[DNA] > 0.5\text{mg/ml}$ as the salt is decreased below 0.01M. 4) The fast mode appears at a higher salt concentration as the DNA concentration is increased. 5) D_{app} and the contribution of the fast mode to the diffusion process both increase with increasing DNA concentration. Studies with higher-valent counterions are under way.

Tu-Pos9

SEQUENCE-DEPENDENCE OF DIVALENT CATION
BINDING ENVIRONMENTS ON DOUBLE-HELICAL DNA.

W. Braunlin*, L. Nordenskiöld', and

T. Drakenberg[§]. *Dept. of Chemistry, Polytechnic University, Brooklyn, NY. 'Dept. of Physical Chemistry, University of Stockholm. [§]Dept. of Physical Chemistry 2, Lund University, Lund, Sweden.

Based on ^{43}Ca NMR chemical shift and relaxation measurements, the number of strong Ca^{2+} sites on natural double-helical DNA increases sharply with increased GC content. Synthetic polynucleotides show no corresponding evidence of binding heterogeneity. However, large differences are observed in bound $^{43}\text{Ca}^{2+}$ shifts and relaxation rates among the polynucleotides studied. Thus, local DNA structure seems to be a strong determinant of Ca^{2+} binding.

Comparing ^{43}Ca and ^{25}Mg NMR results, Ca^{2+} and Mg^{2+} seem to recognize similar structural features on DNA.

Tu-Pos11

ENTROPIES AND ENTHALPIES OF PHASE TRANSITIONS IN LIPIDS AND NUCLEIC ACIDS THROUGH DIRECT MEASUREMENT OF FREE ENERGIES.

Adrian Parsegian, Donald Rau, NIH Bethesda, MD
Peter Rand, Nola Fuller, Brock Univ., St Catherines, Ont.

Ever since the development of the Clausius-Clapeyron Equation long ago, all the scientific world has been keenly aware of the close connection between the heat or entropy of a first-order transition and the sensitivity of the transition temperature T to applied pressure P . Indeed, the entropies and enthalpies derived from dP/dT are thermodynamically far more rigorous in principle, and often more accurate, than those inferred from calorimetry based on many convenient assumptions. We have recently generalized the Cl-CI Equation to apply to changes in lipid or DNA transitions with osmotic stress. We have mapped the main hydrocarbon phase transition of DLPC as well as the ordering transition in DNA assemblies. This information allows a far more thorough characterization of the transition than has been available hitherto and a far more rigorous test of phase transition models than previously possible. We have, in like manner, learned to convert force vs. distance curves into the entropy and enthalpy vs. separation of DNA macromolecules. A return to the fundamental origins of these interactions allows much more critical thinking about molecular interaction and assembly.

Tu-Pos10

C-13 NMR STUDIES OF POLYAMINE BINDING,
MOBILITY, AND DIFFUSION IN DNA SOLUTION.

A. Rehman*, W. Braunlin*, L. Nordenskiöld'

and P. Stilbs[§]. Intro. by N. Tooney*. *Dept. of Chemistry, Polytechnic University, Brooklyn, NY. 'Dept. of Physical Chemistry, University of Stockholm. [§]Dept. of Physical Chemistry, Royal Technological University of Stockholm.

C-13 labelled polyamines and methylated polyamine analogs have been synthesized. The equilibrium binding of these oligocations to DNA has been studied by NMR chemical shift and relaxation measurements. The NMR relaxation measurements also provide a probe of oligocation mobility in DNA solution, and the extent to which steric effects influence this mobility.

Pulsed field gradient NMR diffusion measurements (^1H -1 and C-13) have been performed on polyamines and methylated polyamines in DNA solutions. Polyamine diffusion appears to be sensitive to localized binding.

Tu-Pos12

CHANGES IN SPECIFIC VOLUME AND COMPRESSIBILITY ASSOCIATED WITH THE THERMAL DENATURATION OF DNA. Yun-Xing Wang and Don Eden, Dept. of Chemistry and Biochemistry, San Francisco State Univ., San Francisco, CA 94132.

We have used a temperature scanning instrument that precisely measures the density and sound velocity of solutions to determine the specific volume and adiabatic compressibility of dilute solutions of nucleosomal DNA. Measurements on solutions prepared under isopotential conditions in 1, 5 and 10mM sodium phosphate buffers were made for temperatures between 25 and 80°C. Both the specific volume, \bar{v} , and partial specific adiabatic compressibility, \bar{B}_s , increase with increasing ionic strength and temperature. After correcting for the Donnan terms and using the value of 25 H_2O 's/nucleotide we estimate the average density of the water of hydration at 25°C to be approximately 1.08 g/ml, decreasing with increasing ionic strength. Melting of dsDNA results in a change in \bar{v} at T_m of $-.024 \text{ ml/g}$ in 1mM NaPi and smaller decreases at higher ionic strengths. Melting of dsDNA also results in a decrease in \bar{B}_s which is largest in 1mM NaPi. Supported by USPHS grant GM31674.

Tu-Pos13

FLUORESCENCE CHARACTERISTICS OF OLIGONUCLEOTIDES OF DEFINED BASE SEQUENCE MODIFIED COVALENTLY WITH BaPDE STEREOISOMERS

M. Cosman, V. Ibanez, and N. E. Geacintov, Chemistry Department, New York University, New York, NY 10003

In order to study the effects of base sequence on adduct characteristics derived from the covalent binding of the (+) and (-) enantiomers of BaPDE (*trans*-7, 8-dihydroxy-*anti*-9, 10-epoxy-7, 8, 9, 10 tetra hydrobenzo[a]pyrene), pairs of complementary oligodeoxyribonucleotides 9 to 11 bases long were synthesized. In the case of single-stranded oligonucleotides of different base sequences modified either by (+) or (-) BPDE, the fluorescence excitation and emission profiles of the pyrenyl residues are similar. However, when the complementary strands are added to the unmodified oligonucleotides, a new broad emission band centered at 455 nm appears only in the case of the oligomers modified by the (-) enantiomer. This suggests that considerable ground state pyrenyl residue-base stacking interactions occur in the case of (-)-BPDE, but not (+)-BPDE. These differences in adduct structures could be related to the differences in the biological activities of these two BPDE stereoisomers.

Tu-Pos15

PHYSICAL STUDIES OF STRUCTURAL EQUILIBRIA WITHIN PERIODIC POLY dA-POLY dT SEQUENCES

Shirley Chan, Ken Breslauer: Rutgers Univ
Mike Hogan, Baylor College Medicine
Bob Austin, Jeff Ojemann, Jon Passner and
Nada Wiles: Princeton Univ.

We have studied the temperature dependent conformational changes of poly dA-poly dT sequence elements, in fractionated polymers and in kDNA, employing a combination of physical methods. Circular dichroism reveal a conformation change with 37 C midpoint. Singlet depletion anisotropy and electric birefringence show that the rotational dynamics of dA-dT also display strong changes near 37 C not seen in other sequences. The kDNA fragment displays a similar effect. We conclude that dA-dT sequences as short as 4 basepairs are capable of a temperature equilibrium between 2 helical states. Analysis of the kinetic orientation decay data indicate that dA-dT is very stiff torsionally but soft for bending. Comparison with expected elastic properties of the helix will be made, and the phenomena of bent DNA will be discussed.

Tu-Pos14

COMPOSITION DEPENDENCE OF THE TORSIONAL RIGIDITY OF DNA. RELEVANCE TO THE AFFINITY OF 434 REPRESSOR FOR DIFFERENT OPERATORS. B. S. Fujimoto and J. M. Schurr, Department of Chemistry, University of Washington, Seattle, WA 98195.

Upper and lower bound torsion constants for linear DNAs containing 34 to 100% G-C have been determined by time-resolved measurements of the fluorescence polarization anisotropy (FPA) of intercalated ethidium. A method is presented for determining the actual torsion constant from its lower bound together with the dynamic persistence length, when the latter is known. The torsion constant is observed to depend only slightly, if at all, on base composition over the range examined. The present results are not consistent, either qualitatively or quantitatively, with recent proposals that sequence-dependent variations in the affinity of 434 repressor for different operators are due to composition-dependent variations in their torsional rigidities. For this and other reasons, it seems premature to discount the possibility that sequence-dependent equilibrium structure or bending rigidity of the operator may be important determinants of the binding affinity of 434 repressor for different operators.

Tu-Pos16

AN EPR PROBE TO DETECT LOCAL Z-DNA CONFORMATIONS. O. K. Strobel, R. S. Keyes, and A. M. Bobst, Department of Chemistry, University of Cincinnati, Cincinnati, Ohio 45221.

The spin labeled deoxycytidine triphosphate (pppDCAT) has been incorporated with *Micrococcus luteus* DNA Polymerase to give an EPR active (dG-dC, DCAT), alternating copolymer. In high salt (4.5 M NaCl), (dG-dC, DCAT), gives an EPR spectrum which reflects a significantly different DNA conformation than the one observed in low salt. As a control, the analogous spin labeled polymer (dA-dT, DUAT), resulting from incorporation of the deoxyuridine triphosphate analog (pppDUAT) into (dA-dT), has essentially the same EPR spectrum under high and low salt conditions. Thus, pppDCAT is the first EPR probe capable of detecting Z-DNA. Analyses of the EPR spectra with the Disc Motional Model, which has been successfully applied to nitroxide labeled bases containing tethers of intermediate and low rigidity, indicate a slower motion for dG-dC base pairs in Z-DNA than in B-DNA. Supported in part by NIH GM 27002.

Tu-Pos17

SPECIFIC BINDING OF CRO REPRESSOR TO THE OPERATOR DNA IS CONTROLLED MOSTLY BY ENTHALPIC COMPONENTS. Yoshinori Takeda¹, Philip D. Ross² and Courtney P. Mudd³; ¹Laboratory of Molecular Biology, NCI-FCRF, PRI, Frederick, Maryland 21701, ²Laboratory of Molecular Biology, NIDDK, NIH, Bethesda, Md. 20892, ³Biomedical Engineering and Instrumentation Branch, DRS, NIH, Bethesda, Md. 20892.

We have determined the changes in enthalpy upon formation of Cro-DNA complexes between 10 and 37°C using a pulsed-flow microcalorimeter. Twenty-one base pair DNA duplexes of desired sequences were used. (1) The ΔH upon the formation of the specific Cro repressor-OR3 operator DNA complex (OR3 operator is the strongest binding site for Cro repressor) is endothermic below 15°C and exothermic above 15°C. (2) The ΔH accompanying the formation of the nonspecific DNA complex shows a similar temperature-dependency profile, but, in this case, the ΔH changes its sign at about 30°C. The ΔH 's accompanying the formation of other specific DNA complexes fall in between. (3) The differences in the ΔH 's between the specific OR3 complex and the nonspecific complex are about -6 kcal/mol. Since the difference in free energy change between the specific OR3 complex and the nonspecific complex is also about -6 kcal/mol, it seems that most of the ΔG gained upon the formation of the specific complex is derived from enthalpy change. This is most probably the result of formation of sequence specific H-bonds and hydrophobic interactions between amino acids of Cro and DNA bases when Cro forms the specific complex. We are currently examining ΔH for each sequence specific H-bond and hydrophobic interaction.

Tu-Pos19

THERMODYNAMICS OF HAIRPIN FORMATION: EFFECT OF TEMPERATURE AND PRESSURE.

Robert B Macgregor Jr¹ & Luis A Marky²

¹Molecular Biophysics Research Department, AT&T Bell Laboratories; ²Department of Chemistry, New York University.

DNA complexes formed by synthetic oligomers can provide detailed structural and dynamic information about nucleic acid secondary and tertiary structure. Of special interest are hairpin structures, which have been implicated as binding sites and control regions in DNA duplexes. We have examined the pressure and ionic strength dependence of the UV and CD melting curves as well as performed DSC on the hairpin \rightarrow coil transition of several oligomers. These results will be discussed in terms of available thermodynamic and structural data.

(Supported in part by NIH grants GM 42223 and BRSR S07 RR 07062 to LAM).

Tu-Pos18

EXCITED-STATE PROPERTIES OF DNA

S. Georgiou, G. Ge, R. Weidner, S. Zhu and C.-R. Huang, Physics Dept., Univ. of Tenn., Knoxville, TN (Intr. by P. P. Constantinides)

We have used steady-state and time-resolved fluorescence techniques to study the excited-state properties of oligo- and polynucleotides at room temperature. These properties include (i) the nature of the emitting species, (ii) exciplex formation, (iii) the conformational flexibility of the double helix (monitored using the intrinsic fluorescence of the bases), and (iv) transfer of excitation energy along the helix. With regard to (iv), we find that the experimental results can be simulated by using a stochastic model based on the dipole-dipole approximation for intrastrand transfer between nearest neighbors. The results of this study shed light on the structure and dynamics of nucleic acids and on the generation of stable photoproducts. (Supported by NIH grant GM38236.)

Tu-Pos20

ENHANCED RESOLUTION OF DNA RESTRICTION FRAGMENTS-A PROCEDURE BY 2D ELECTROPHORESIS AND DOUBLE-LABELING. M. Yi, L-C. Au, N. Ichikawa, and P. Ts'o, Div. of Biophysics, School of Hygiene and Public Health, The Johns Hopkins Univ., Baltimore, MD 21205

A probe-free method was developed to detect DNA rearrangement based on the separation of restriction fragments of genomic DNA generated by two enzymatic digestions in a 2D electrophoresis (elec.) pattern. After the first D elec. of the first enzymic digest obtained in solution, the second digestion was carried out in the gel and followed by the second D elec. The DNA restriction fragments were separated into a map with x-y coordinates, consisting of 300-400 spots. The test DNA and the reference DNA were labeled by ^{35}S and ^{32}P respectively, and the gel was exposed to two x-ray films, with the upper film receiving only the ^{32}P emission and the lower film receiving both ^{32}P and ^{35}S emission. Appropriate photographic procedure allows only the different DNA fragments to be shown in the 2D photo map. The comparison between the DNA fragments from *E.coli* HB101 (λ) and *E.coli* HB101 was used to demonstrate the identification of the incorporation of λ DNA in the *E.coli* genome in this study. (Supported in part by DOE)

Tu-Pos21

IMAGING OF KINKED CONFIGURATIONS OF DNA MOLECULES UNDERGOING OFAGE USING FLUORESCENCE MICROSCOPY

Carlos Bustamante and Sergio Gurrieri
Department of Chemistry, University of New Mexico, Albuquerque, N.M.: 87131

The dynamics of individual DNA molecules undergoing OFAGE (Orthogonal Field Alternating Gel Electrophoresis) has been studied using T2 DNA molecules labelled with a dye and visualized with a fluorescence microscope. The mechanism of reorientation of the molecules in the direction of the new orthogonal field, depends on the degree of extension of the chain immediately before the application of this field. Kink formation is promoted when time is allowed between the application of the two orthogonal fields so that the molecules attain a partially relaxed configuration. In this case, the chains appear bunched up in domains moving along the contour of the molecule. These regions are the locations where the kinks are formed upon application of the second orthogonal field. The formation of kinks provide a significant retardation of the reorientation of the molecules, relative to molecules that do not form kinks, and might play an important role in the fractionation attained with OFAGE. The various re-orientation mechanisms observed in the molecules are classified.

Tu-Pos22

Ligand Binding Studies in Myoglobin using Temperature-Derivative Spectroscopy.

Joel Berendzen & David Braunstein

U. of Ill. at Urbana-Champaign, Urbana, IL 61801.

We present results on the dynamics of CO binding to sperm-whale myoglobin during and after photolysis. New measurements of the infrared CO stretch bands ($1900\text{--}2200\text{ cm}^{-1}$) at low temperatures corroborate earlier results showing distributed activation enthalpies with different distributions for each band, transfer between two bands that correspond to photolyzed ligands, and kinetic hole-burning. Using a method that measures the derivative of a population with respect to temperature, we are able to show that the geminate process may be described by gaussian enthalpy distributions and to calculate the widths of each distribution.

Novel experiments combining Temperature-Derivative Spectroscopy with continuous photolysis reveal details about the processes by which ligands leave and reenter the heme pocket. Analysis yields information about the barriers to recombination from outside the pocket and the barriers to exchange among conformational substates of the bound protein.

These types of experiments, which rely upon the temperature-dependence of rates, should have applicability to a wide variety of other spectroscopies and proteins.

This work was supported by NSF grant DMB82-09616 and NIH grants GM18051 and GM32455.

Tu-Pos24

X-RAY STUDIES OF CYTOCHROME *c* AT LOW IONIC STRENGTH. M. Walter, S. Watowich, E. Westbrook, and E. Margolia. Dept. of Biochem. and Molecular Biology, Northwestern University, Evanston, Illinois 60208

Crystallographic studies of cytochrome *c* have been initiated to study the effect of ionic strength upon the protein's structure. Visible, Raman, and NMR spectroscopy as well as small angle X-ray scattering suggest that the structures at high and low ionic strength are not identical. In contrast to previous crystallization conditions, which require an ionic strength of 7.5 M, we have successfully crystallized both the ferri- and ferrous tuna proteins as well as those from horse and yeast, at an ionic strength of 45 mM, making it possible to determine the structure of cytochrome *c* under the same conditions employed to characterize its function. The 2.8 Å structure for the tuna ferricytochrome *c* crystals was solved by molecular replacement and refined by least squares methods to an R value of 24%. We are currently improving the stereochemistry. The packing arrangement in these low ionic strength crystals preserves a portion of the contacts present at high ionic strength but introduces contacts novel to the low ionic strength environment. When compared with the high ionic strength structure, significant movement is seen in both surface and heme region residues. (NIH grants AI-12001 and GM-19121 and DOE contract W-31-109-ENG-38)

Tu-Pos23

pH - induced conformational changes of the iron - His(F8) - interface in deoxyhemoglobin - trout IV as detected by the Raman active Fe^{2+} - His(F8) - stretching mode.M. Rosenbeck, R. Schweitzer-Stenner and W. Dreybrodt
University of Bremen, Physics Department,
2800 Bremen 33, Fed. Rep. of Germany

We analysed the O₂-binding isotherms of Hb trout IV using the Herzfeld-Stanley model. Among others the model reveals the existence of different titration states of the subunits due to the protonation of alkaline Bohr groups. In order to probe how these protonations affect the heme-protein interactions we have measured the line profile of the Fe^{2+} -N₅ (His(F8)) - Raman mode of deoxyHb - trout IV at various pH - values. The experimentally observed Raman profiles were decomposed into five different Raman lines with frequencies of 205 cm^{-1} , 212 cm^{-1} , 218 cm^{-1} , 220 cm^{-1} and 225 cm^{-1} . Their intensities depend significantly on pH. We formulated a titration model relating each protonation state determined by the occupation of Bohr groups ($\text{pK}_a=8.5, 8.4$; $\text{pK}_a=7.5, 7.4$) to one of the five Fe^{2+} -His(F8) lines obtained. The intensity of those lines then reflect the pH - dependence of the molar fractions of the involved titration states. Fitting this model to the pH - dependent intensities of the five Fe^{2+} - His (F9) lines yields a good reproduction of the experimental data. We therefore conclude that proton binding to Bohr groups influences the heme along the iron - histidine linkage.

Tu-Pos25

MODULATION OF THE PLANARITY OF TETRAPYRROLES AND ITS FUNCTIONAL REPERCUSSIONS*
John A. Shelnutt, Fuel Science Division 6211, Sandia National Laboratories, Albuquerque, NM 87185

Non-planar tetrapyrrole structures are suggested to play a role in photosynthetic reaction centers and in B₁₂-dependant enzymes. Non-planar structures of the nickel-tetrapyrrole cofactor F₄₃₀ of methylreductase may play a role in that enzyme's biological function by allowing the macrocycle core to expand and contract as the Ni ion cycles between oxidation states. The planarity of F₄₃₀ is also proposed to affect axial ligand affinity, suggesting the possible regulation of affinity by protein control of macrocycle planarity. Raman studies show that four-coordinate Ni(II) tetrapyrroles in solution are present in an equilibrium mixture of planar and ruffled conformers. This is true for nickel octaethylporphyrin, protoporphyrin, uroporphyrin (NiUroP), and a corphinate related to F₄₃₀ of methyl-coenzyme M methylreductase. We have shown that macrocycle planarity influences axial ligand affinity for epimers of F₄₃₀ and for Ni porphyrins. For example, binding of nickel protoporphyrin to apohemoglobin results in only the planar conformer, which has high affinity for the proximal histidine; however, reconstituted α chains admit non-planar conformers with lower affinity. Like globin binding, π - π complex formation and dimerization of Ni porphyrins affect macrocycle planarity. Finally, the transient change in planarity in the excited state of NiUroP perturbs the ring stacking in some π - π complexes. An overview of recent Raman studies will be given.

*Supported by U.S. Department of Energy Contract DE-AC04-76DP00789 and GRI Contract 5082-260-0767.

Tu-Pos26

IONIC STRENGTH DEPENDENCY OF THE ELECTRON TRANSFER FROM CYTOCHROME c TO CYTOCHROME c OXIDASE. James T. Hazzard, Shouyu Rong, and Gordon Tollin. Department of Biochemistry, University of Arizona, Tucson, Arizona 85721

The effect of ionic strength on the intramolecular one-electron reduction of cytochrome c oxidase (CcO) by cytochrome c has been studied using flavin semiquinone reductants generated *in situ* by laser flash photolysis. In the absence of cytochrome c, direct reduction of CcO by the one-electron reductant 5-deaza-riboflavin semiquinone occurs slowly. Addition of cytochrome c results in a marked increase in the rate and amount of reduced CcO generated per laser flash. Reduction of CcO at the cytochrome a site is monophasic, whereas oxidation of cytochrome c is multiphasic, the fastest phase corresponding to the reduction of cytochrome a. A first-order rate-limiting process controls electron transfer to the cytochrome a which has a marked ionic strength effect, with a maximum rate constant occurring at $I = 110 \text{ mM}$. Work supported by NIH Grant DK15057 (to G.T.).

Tu-Pos28

A COMPARISON OF APO AND DesFE MYOGLOBIN USING NMR SPECTROSCOPY M.J. Cocco and J.T. Lecomte, Chemistry Department, Penn State University, University Park, PA 16802.

Apomyoglobin (apoMb) has less helicity, compactness, and stability than holomyoglobin¹. It forms with protoporphyrin IX (PrIX) a complex (desFe Mb) which has a conformation similar to that of the holoprotein². Thus, the PrIX ring and not the iron appears necessary to complete the folding of holo Mb. We investigated the conformational changes induced by PrIX on apoMb and the precise structural role played by the Fe atom. By comparing 2D NMR results obtained on these two proteins, we were able to define several essential stabilizing interactions in each. For example, similarity between the Trp 14 local environments was taken to imply that elements from the A, B, and H helices are in close proximity in apoMb as well as desFe Mb. Hence, this stable core is minimally perturbed by the binding. Other results, bearing on the binding site, were also obtained. (Supported by ACS-PRF 20334-G3).

¹Griko, Yu. et al., *J. Mol. Biol.* **1988** 202 127.

²Breslow, E. et al., *J. Biol. Chem.* **1967** 242 4149; and our unpublished NMR data.

Tu-Pos27

CO BINDING BY THE MULTHEME CYTOCHROME C3: FLASH PHOTOLYSIS AND FTIR STUDIES. J. H. Hazzard, W. Goretski, R. Bartsch and M. A. Cusanovich. Department of Biochemistry, University of Arizona, Tucson, Arizona 85721.

The CO binding properties of a low potential single subunit protein, cytochrome c₃, have been investigated as a means of identifying differences among the four heme environments which are related to their differing redox potentials (ranging from -240 to -381 mV). Flash-induced CO rebinding to the cytochromes isolated from *Desulfovibrio vulgaris* Hildenborough and *Desulfovibrio desulfuricans* Norway exhibits multiphasic second-order kinetics. FTIR spectra indicate the presence of multiple CO ligand conformations at each heme. Assignments of individual hemes to the kinetic phases and CO bands will be presented and discussed.

Supported by the Office of Naval Research.

Tu-Pos29

STRUCTURAL CHARACTERIZATION OF APOCYTOCHROME b₅ BY PROTON NMR SPECTROSCOPY C.D. Moore and J.T. Lecomte, Chemistry Department, Penn State University, University Park, PA 16802.

Extraction of the prosthetic group from b-heme-proteins generally entails partial loss of stability, compactness, and native fold. We are studying the apoprotein of the soluble fragment of rat liver cytochrome b₅ by ¹H NMR; this protein is used as a model for the influence of the heme group on the polypeptide conformation. The aromatic resonances, including those from the six histidines, were identified by 2D NMR methods. Sequence specificity was achieved by comparing the NOEs detected in the apoprotein with those in the reduced holoprotein and those expected based on the crystal structure. These comparisons also led to the assignment of the high field methyl resonances. Thus, we have been able to identify several hydrophobic residues clustering around the only Trp. Nearby, but not included in this cluster, is His 15. A study of the pH response for this residue showed an abnormally high pK_a, implying an environment which stabilizes the protonated form. The behavior of the other His sidechains was also interpreted in structural terms.

Tu-Pos30

THE PROGRESS OF HEMOGLOBIN S GELATION UNDER SHEAR AND THE KINETICS OF DEVELOPMENT OF THE VISCOUS AND ELASTIC COMPONENTS OF COMPLEX VISCOSITY. R.E. Samuel, H.J. Meiselman & R.W. Briehl. Albert Einstein College of Med., Bronx, NY & Univ. So. California School of Med., Los Angeles, CA.

Gelation of HbS proceeds exponentially as observed by cone-plate viscometry. The exponential rate increases in approximate proportion to the first power of shear rate. The rate has a high concentration dependence which decreases as shear rate increases. In a capillary viscometer at 2 Hz elastic and viscous components progress in parallel and at the same exponential rates. The shear dependence of rates is the same as in simple viscosity. The early appearance of elasticity and its progress parallel to viscosity is consistent with the early existence of a gel, as in our direct observations on fibers in real time (Samuel et al, these abstracts). It is not consistent with independent fibers in solution. The first power dependence of rate on shear disfavors breakage of independent fibers as a mechanism for the shear induced acceleration. The acceleration may be due to enhanced nucleation and/or perturbation or breakage of the gel network. (Supported by NIH grants HL 07451 & HL 41341).

Tu-Pos32

PHOTOACOUSTIC STUDIES OF CARBOXYMYOGLOBIN

Shane L. Larson and Jeanne Rudzki Small

Department of Biochemistry & Biophysics
Oregon State University, Corvallis, OR 97331-6503

Pulsed-laser photoacoustics offers a means for measuring the Fe-CO bond strength in carboxymyoglobin, as well as the dynamics of the protein following cleavage of the Fe-CO bond. Two groups have studied the problem in the past, with conflicting results [Leung *et al.*, Chem. Phys. Letts. **141**, 220 (1987); Westrick *et al.*, Biochemistry **26**, 8313 (1987)]. Preliminary results from our laboratory support a positive value for the enthalpy of formation of the Fe:CO geminate pair, formed within 10 nsec of photolysis of carboxymyoglobin. Data will be presented on the Fe-CO bond energy, and the volumetric and enthalpic changes which occur in myoglobin following Fe-CO bond cleavage.

Supported by NIH grant GM-41415.

Tu-Pos31

DIRECT OBSERVATION OF NUCLEATION, GROWTH AND GELATION OF SICKLE CELL HEMOGLOBIN (HbS) BY VIDEO ENHANCED DIFFERENTIAL INTERFERENCE CONTRAST (DIC) MICROSCOPY. R.E. Samuel, E.D. Salmon & R.W. Briehl. Albert Einstein College of Medicine, Bronx, NY & Univ. of N. Carolina, Chapel Hill, NC.

Real time observations (video to be shown) on deoxyHbS at 28° and 13 mM (heme) in 0.1 M phosphate show fibers growing at about 0.3 micron/sec. The fibers are long, reaching lengths in the millimeter range. Fibers develop thick regions (corresponding to a double or multiple fiber) which grow and then branch to form new fibers. This is heterogeneous nucleation of the double nucleation model (Ferrone et al, J. Mol. Biol. **183**:611, 1985). Rare centers with many radiating fibers correspond to "homogeneous" nuclei. Cross-links to form a network occur (beginning very early) due to (a) branching, (b) lateral association of fibers and (c) formation of fixed X-shaped junctions between fibers. Hence the system is a gel even early in polymerization. Fibers are highly flexible, bend greatly and oscillate with Brownian motion. Severing of fibers with a UV beam results in growth at about equal rates at both cut ends. (Supported by NIH grant HL 07451).

Tu-Pos33

RESONANCE RAMAN STUDIES OF THE INTERACTION OF MESOHEME AND COPPER WITH HISTIDINE-RICH GLYCOPROTEIN

BB Muhoberac,¹ RW Larsen,² DJ Nunez,² WT Morgan³ and MR Ondrias². ¹Dept of Chem, IUPUI, Indianapolis, IN 46205, ²Dept of Chem, U of NM, Albuquerque, NM 87131 and ³Div of Biochem and Molec Biol, U of MO, Kansas City, MO 64110
Histidine-rich Glycoprotein (HRG) binds hemes and a variety of metal ions. Optical absorption and EPR spectra of the mesoheme-HRG complex exhibit changes upon copper and ligand binding that can be elucidated further by heme-specific spectroscopy. Resonance Raman spectra show that Fe³⁺-mesoheme-HRG changes spin state during the titration from 0 to 20 equivalents of Cu²⁺. Specifically, ν_2 shifts from 1594 to 1583 cm⁻¹ and ν_3 from 1506 to 1493 cm⁻¹ indicative of a low- to high-spin transition from a 6 to 5 coordinate complex, and the 1475 cm⁻¹ marker for high-spin, 6 coordinate heme is not detected. In contrast, Fe²⁺-mesoheme-HRG shows ν_2 at 1600 cm⁻¹ and ν_3 at 1493 cm⁻¹, which are characteristic of low-spin heme, independent of the presence of Cu¹⁺. Furthermore, the low frequency spectrum displays no iron-histidine stretch suggesting a 6 coordinate complex. CO-bound Fe²⁺-mesoheme-HRG exhibits an unusually broad iron-CO stretch at 507 cm⁻¹ implying inhomogeneity in the CO orientation. These studies will be used to discuss axial ligation and heme pocket interactions in the cardiac cytochrome oxidase and other hemeproteins.

Tu-Pos34

FLUOROMETRIC STUDIES ON THE ACTIVE SITE CONFORMATION OF CYTOCHROME P450.

Yoshiaki Omata and Fred K. Friedman, National Cancer Institute, National Institutes of Health, Bethesda, MD 20892.

We utilized the fluorescence of the substrate benzo[a]pyrene (BP) as a probe of the active site conformation of cytochrome P450. The fluorescence of BP in the substrate binding site is quenched by excitation energy transfer from BP to the heme of P450 and depends on the distance and/or orientation between BP and heme. Fluorescence of the BP-P450c complex was further quenched by addition of NADPH-cytochrome P450 reductase, which interacts with P450 during its catalytic cycle. This quenching arises from a change in the spatial relationship between BP and heme and indicates that reductase alters the active site conformation. The quenching data revealed that reductase forms an equimolar complex with P450c. In the presence of monoclonal antibody 1-7-1, which inhibits hydroxylation of P450c, reductase had no effect on fluorescence. Antibody binding to P450c therefore interferes with the reductase-induced change in the active site conformation.

Tu-Pos36

INVESTIGATING THE ROLE OF COPPER IN CYTOCHROME *O*: A TERMINAL OXIDASE OF *ESCHERICHIA COLI*

N. Elise Gabriel and Sunney I. Chan, California Institute of Technology, Pasadena, California 91125; and Kimberly Carter Minghetti, Christos D. Georgiou, and Robert B. Gennis, University of Illinois, Urbana, Illinois 61801

Cytochrome *o* is one of two terminal oxidases in the aerobic respiratory chains of *Escherichia coli*. The enzyme catalyses the two electron oxidation of ubiquinol-8 in the cytoplasmic membrane and reduces molecular oxygen to water. Electron flow through the cytochrome *o* complex generates a proton motive force both *in vivo* and *in vitro*. Several purification protocols have been reported for cytochrome *o*, and the enzyme has been claimed to have either two or four subunits. An improved isolation procedure from an overproducing strain of cytochrome *o* complex is reported. Starting from membranes, the enzyme can be purified following solubilization in detergents and one column chromatography step. The resulting oxidase has four subunits and high ubiquinol oxidase activity. The composition and spectroscopic properties of the pure enzyme are comparable to enzyme isolated in other laboratories. The enzyme complex contains two mol protoheme IX as well as copper. EPR characterization of the isolated enzyme shows that one heme is a high spin species, while the other is low spin. One copper is easily denatured and removable. This result does not affect enzymatic activity, but may be related to the fact that isolated cytochrome *o* reconstituted in vesicles does not pump protons unlike its mammalian counter part, cytochrome c oxidase.

Tu-Pos35

EFFECT OF ANIONS AND TEMPERATURE ON THE OXYGEN EQUILIBRIUM OF BOVINE HEMOGLOBIN
A. Razynska, C. Fronticelli, E. Bucci, E. Di Cera, K. Gryczynski. Dept. Biochem. U. MD at Baltimore 21201 and U. Cattolica. Rome, Italy

Measurements of the oxygen binding to bovine Hb have been carried out over a wide range of Cl⁻ and Br⁻ concentrations. Br⁻ has higher affinity for both the deoxy and oxy forms of bovine Hb with respect to Cl⁻. The free energy of linkage related to the change in anion affinity observed in the deoxy oxy transition is, however, smaller in the presence of Br⁻. The effect of temperature on oxygen equilibria has been studied in the temperature range of 15-37°C at pH 7.4. The standard enthalpy of oxygenation is found to be -8.22 Kcal/mol in the presence of 0.1 M chloride and -8.94 Kcal/mol in the presence of 0.1 M bromide. Corrections of these values for the heat of solution of oxygen and the heat of Bohr proton release yields a value of "intrinsic" heat of oxygenation of about -7.8 Kcal/mol. In similar conditions, the intrinsic heat of oxygenation measured for human Hb was -14.1 Kcal/mol.

Tu-Pos37

CO BINDING KINETICS AND QUATERNARY TRANSITIONS IN HEMOGLOBIN VALENCE HYBRIDS

John S. Philo, Ulrich Dreyer, & Jeffrey W. Lary. Molecular & Cell Biology, University of Connecticut, Storrs, CT 06269

We have studied CO binding after laser photolysis in symmetric valence hybrids of human Hb, while varying the sixth ligand on the ferric subunits. Our goal is to investigate the role of the spin state of the ferric subunit in determining the overall quaternary structure, and conversely the extent to which changes in quaternary structure cause shifts in the spin equilibria of mixed-spin ferric forms. Both optical and time-resolved magnetic susceptibility data were collected for CN⁻, N₃⁻, SCN⁻, aquo, and F⁻ ferric forms of both $\alpha^2\beta^2$ and $\alpha^3\beta^2$ hybrids. For each form, data at several CO concentrations and for full and partial photolysis have been fitted to a kinetic allosteric model which includes the rates of R-T and T-R transitions as well as the CO binding rates for the R and T states. The view that valence hybrids are largely non-cooperative and have slow conformational equilibria has been strongly biased by the common use of only the CN⁻ form. Except for the CN⁻ forms, full photolysis yields substantial switching from the R to T state in $\approx 10^{-4}$ s. The R-T rates can be deduced from the characteristic spectral changes in the deoxy hemes, as well as from competition between CO rebinding and R-T transitions at high CO concentrations. The CN⁻ hybrids are anomalous, with a small fraction locked in a very slow quaternary equilibrium.

While higher spin ferric ligands do generally give more T state, neither the allosteric constants nor R-T rates vary systematically with spin state as predicted by the Perutz stereochemical model. The time-resolved magnetic data also show that the R-T switch produces only small shifts in the spin equilibria of the ferric subunits.

Supported by NIH (HL-24644) and NSF (PCM 79-03964 & 82-11437).

Tu-Pos38

STABILITY AND AUTOXIDATION OF CROSSLINKED HEMOGLOBINS. Thao Yang, Qun-Ying Zhang, Susan M. Bauer, Timothy R. Filley, Sonali Dave and Kenneth W. Olsen; Department of Chemistry, Loyola University of Chicago, 6525 N. Sheridan Rd., Chicago, IL 60626.

Human Hb A has been stabilized by bis(3,5-dibromosalicyl) fumarate (diaspirin), dimethylpimelimidate (DMP), bis(β -chloroethyl) methylamine (BCEA) and tris(β -chloroethyl)amine (TCEA). The absorbance changes were monitored spectrophotometrically while heating the sample at 0.3°C/min from 24–70°C. Hemoglobin crosslinked by diaspirin between the two Lys β 82's or Lys α 99's have a markedly higher T_m of 57°C, while the T_m of Hb A is 41°C. Hb A crosslinked with TCEA has a T_m of 49°C, but BCEA crosslinking does not raise the T_m of Hb A (41.3°C). The Hb A treated with DMP has a T_m of 56°C. The β 82 and α 99 crosslinked oxy Hb A were further treated with DMP to produce double crosslinked hemoglobins, which have a T_m of 60°C. The autoxidation rate of α 99 crosslinked Hb A was 1.8 and 1.5 fold faster than those of Hb A and β 82 crosslinked Hb A, respectively. Catalase and superoxide dismutase could each decrease these autoxidation rates by 2 fold. These results should improve the design of stabilized crosslinked hemoglobins as blood substitutes. (Supported by a grant from the American Heart Association of Metro. Chicago.)

Tu-Pos40

THE IMPORTANCE OF CHARGE COMPLEMENTATION TO REACTIONS BETWEEN CYTOCHROME C2 AND PHOTOSYNTHETIC REACTION CENTERS. Michael Caffrey and Michael Cusanovich. Dept. of Biochemistry, University of Arizona, Tucson, AZ 85721.

To test the importance of charge-charge interactions to reactions between soluble cytochromes c and their physiological partners, we have prepared a number of site-directed mutations to basic residues surrounding the exposed heme edge of *R. capsulatus* cytochrome C2. We have examined the effects of changing the sign of the charge at three positions (K12D, K14E and K32E). In addition, we have constructed a double charge mutation (K14E/K32E). The ionic strength dependence of first and second order reactions of flash-activated *R. sphaeroides* photosynthetic reaction centers and reduced cytochromes C2 have been examined. We will show that there are distinct kinetic differences between the wild-type cytochrome and the charge mutations. Furthermore, we find substantial kinetic differences between the various charge mutations. It is anticipated that these results will allow us to model the molecular contacts between cytochrome C2 and reaction centers at high resolution and to directly measure the effect of electrostatic interactions on transient complex formation. Supported by USPHS GM 21277.

Tu-Pos39

QUANTITATION OF THE BINDING OF OXYGEN TO HUMAN HEMOGLOBIN. L. J. Parkhurst, T. M. Larsen, and T. C. Mueser, Dept. of Chemistry, Univ. of Nebraska, Lincoln, NE 68588-0304.

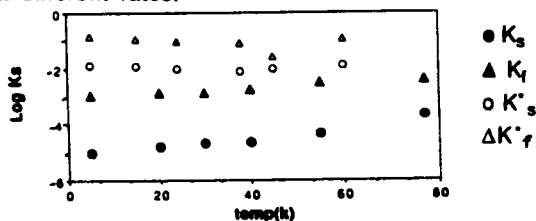
A solution of oxyhemoglobin and oxymyoglobin is flowed rapidly against an enzyme solution in a special stopped-flow apparatus built into the sample compartment of a Cary 210 spectrophotometer. The rapid mixing initiates the slow removal of oxygen from the solution. Absorbance readings are made at the isosbestic wavelength for oxy-deoxy Mb to determine the Hb absorbance isotherm, and at the quasi-isosbestic of Hb to determine the Mb absorbance isotherm from which the oxygen concentration can be calculated since the equilibrium constant for Mb has been precisely determined. Detailed analysis of the enzyme kinetics has allowed precise values for oxygen at early times to be determined. Current efforts are directed toward determining to what extent three additional spectroscopic constants must be precisely determined in addition to the four Adair constants in order to convert the absorbance isotherm into a true binding isotherm.

Grant Support: NIH DK 36288, American Heart Assoc., Neb. Affiliate, Research Council, Univ. of Nebraska.

Tu-Pos41

KINETIC TITRATION OF CONFORMATIONAL SUBSTATES (A New Experimental Approach To Study Non - Exponential Kinetics Of Heme Proteins) K. S. Reddy and B. Chance., Dept. of Biochem. & Biophysics, Univ. of Penn., Phila., PA 19104.

Recently(1), using light and temperature perturbation techniques under equilibrium conditions below 80K, we have presented experimental evidence for the relaxation process in photoproduct before rebinding in the reaction, $Mb^* + CO \rightarrow MbCO$. Of central interest are the results of light jump under background illumination. The isothermal and light jump kinetic data could be fitted in terms of fast (K_f) and slow (K_s) components. The rate constants $K_f(\Delta)$ & $K_s(e)$ are calculated from isothermal kinetic data and $K_f'(\Delta)$ & $K_s'(e)$ are calculated from light jump perturbation profiles. $K_s'(e) > 10^2 K_s(e)$ and $K_f'(\Delta) > 10^2 K_f(\Delta)$. These results are at least two orders of magnitude faster than the isothermal technique. This indicates that the relaxed and unrelaxed photoproduct (Mb^*) recombines at different rates.



(1). K. S. Reddy and B. Chance, Am. Phys. soc. J., 33, 690 (1988), Biophys. J., 55, 555a (1989)

Tu-P042

ENHANCED INTERNAL ELECTRON TRANSFER WITHIN THE SUBUNIT 5B ISOZYME OF YEAST CYTOCHROME OXIDASE.

R.A. Waterland, A. Basu, R.O. Poyton*, B. Chance. Univ. of Penn., Dept. of Biochem/Biophys., Phila., PA 19104

*Univ. of Colorado, Dept. of MCD Bio., Boulder, CO 80309 (Intro. by L. Peachey).

Gene deficient mutants have been utilized to investigate the plausible modulation of oxidase function between the subunit 5 isozymes of yeast cytochrome oxidase. Room temperature turnover number (assayed polarographically), as well as low temperature rates of ligand binding, internal electron transfer (heme a oxidation) and single turnover cytochrome c oxidation (all monitored spectroscopically) were measured within whole cell suspensions of *Saccharomyces cerevisiae*. The wild type (JM43), which incorporates 5a virtually exclusively, was compared with a COX 5a deletion mutant (RP3-F) which synthesizes only the 5b isozyme. Previous measurements of a difference of CO ligation (1) were not confirmed with currently available cells. The rate of ligand binding (CO recombination) is identical for the wild type and mutant oxidase; furthermore, the rate of single turnover of cytochrome c oxidation is likewise unchanged. Internal electron transfer was monitored at 605 nm from -70 to -100 C; the reaction was initiated by photolysis of a CO ligated, O₂ saturated suspension (triple trapping). We have found a difference in the low temperature electron transfer from a to a₃. Semilog plots indicate a biphasic heme a oxidation, the slow phase of which was considered the a to a₃ electron transfer. The electron transfer activation energy of (48 ± 2) Kcal/mol was the same for both the wild type and the mutant, but the overall reaction rate of oxidation of a by a₃ was ~3.5 fold faster within the mutant.

1) Waterland, R. et al (1988) *Faseb J.* 2:A774.

Tu-P044

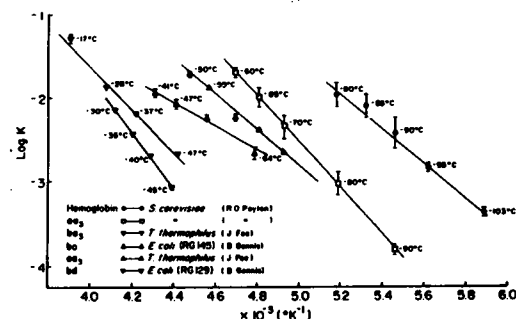
TUNICHLORIN: SPECTROSCOPY OF THE NATURALLY-OCCURRING NICKEL(II)-PYROPHEOPHORIBIDE α COMPLEX AND ITS DERIVATIVES. L.A. Andersson, Oregon Graduate Center, Beaverton, OR 97006; A. Huff, Univ. of South Carolina, Columbia, SC 29205; and K.M. Smith, Univ. of California, Davis, CA 95616.

Tunichlorin (TC) is a novel pyrochlorophyll α derivative isolated from tunicates, that is nickel(II)-substituted and has a 2-hydroxymethyl moiety. We have prepared a series of TC derivatives, where only the C2 substituent is varied (e.g., vinyl, formyl, nitrile, acetyl). The electronic absorption, circular dichroism (CD), and magnetic circular dichroism (MCD) spectra of the complexes differ markedly. For example, in the UV-vis, the B/Q ratio of TC is ~1:1, vs. ~3:1 for metallochlorins or ~20:1 for hemes. Replacing the 2-hydroxymethyl group of TC with a vinyl alters the B/Q ratio to ~2:1; replacing it with a formyl results in a B/Q of 0.75:1. Shifts in band positions are also apparent. In the CD and MCD spectra, both bandshifts and intensity changes are evident. Thus, changes at the C2 position of tunichlorin have a surprisingly large effect on the macrocyclic properties.

Tu-P043

COMPARATIVE BIOCHEMISTRY OF RESPIRATORY PIGMENTS OF CYTOCHROME OXIDASES AND A HEMOGLOBIN. Basu, A., Yin, M. & Chance, B. Dept. Biochem. & Biophys., Univ. of Penn., Phila., Pa. 19104

The plethora of microbial oxidases revealed by photochemical action spectra (Chance, B. 1989 BBA in press) has lead to detailed identification, purification and over production in many species, to the point where kinetic comparison of properties is possible leading ultimately to structure/function deductions. The four types of oxidase and the hemoglobin were obtained from organisms as shown in the figure with appropriate credits. The cell suspensions were reduced to a substrate, saturated with CO and photolyzed at temperatures appropriate to ready measurement of the recombination rate. The results are plotted in an Arrhenius type plot and show a sequence of rates, yeast, hemoglobin, yeast aa3, *E. coli* bo, aa3 of thermophilus, *E. coli* bd and ba3 of thermophilus. The results suggest the CO ligation, analogous to oxygen ligation is a sensitive indicator of the heme environment and heme structure.



Tu-P045

SUBUNIT INTERACTIONS AND ALLOSTERIC EFFECTS IN HEMOGLOBIN: HIGH PRESSURE FLUORESCENCE STUDIES

C. Royer¹, S. Pin^{1,2}, G. Weber³, B. Alpert² & E. Gratton¹. ¹UIUC, LFD, 1110 W. Green St., Urbana, IL 61801; ²Univ. de Paris, Lab. de Biologie Physico-Chimique, 2, Place Jussieu, 75251 Paris; ³UIUC, Dept. Biochem., 1209 W. California, Urbana, IL 61801.

The dissociation of human hemoglobin labeled with the covalent fluorescence dye, 1-5 dansyl, was studied by monitoring the polarization and lifetime of the dansyl emission as a function of concentration and pressure. The apparent rotational volumes extracted from these data were used to indicate the oligomeric state of the protein. Dissociation profiles were obtained for standard hemoglobin as well as for the major component of a further DEAE purification at pH 7 in absence and in presence of the allosteric effector (inositol hexaphosphate) and at pH 9. Our results show a destabilization of the $\alpha_2\beta_2$ tetramer at high pH for both preparations and a stabilization of the tetramer at pH 7 for the major component as compared to the standard preparation. High pressure experiments resulted in hemoglobin monomer formation indicating that the $\alpha_1\beta_1$ interface interactions are weaker than generally assumed. (Supported in part by PHS-P41-RR03155 and French Foreign Ministry.)

Tu-Pos46

THE STRUCTURE OF THE ACTIVE SITE OF NATIVE LIGNINASE AND COMPOUND III.

R. Sinclair¹, L. Powers¹, B. Brock² and J. Bumpus². ¹Center for Bio-Catalysis Science and Technology, ²Biotechnology Center, Utah State University, Logan, Utah 84322.

The wood destroying fungus *Phanerochaete chrysosporium* secretes a number of extracellular enzymes called ligninases which have been implicated in the biodegradation of lignin and numerous persistent environmental pollutants (such as pentachlorophenol). Ligninase isozyme, H2, a glycosylated protein of approximately 40 kD contains a single heme. X-ray absorption spectroscopy (XAS) has been used to probe the local environment of the iron in the active site of resting enzyme and compound III. The results are compared with those obtained from similar studies of both peroxidative and non peroxidative heme proteins including HRP, lactoperoxidase and a peroxidative derivative of cytochrome-c, microperoxidase MP11.

Supported by NIEHS Superfund Grant ES 04922

Tu-Pos48

RELAXATION DYNAMICS IN CARBON-MONOXY HEMEPROTEINS. R. Scholl, S. R. Blanke, K. Chu, D. Ehrenstein, H. Frauenfelder, L. P. Hager, J. B. Johnson, C. Jung⁺, J. R. Mourant, R. Philipp, S. G. Sligar, P. Stayton, Y. J. Suh, R. D. Young; U. of Illinois at Urbana-Champaign.*

— Using FTIR spectroscopy to monitor the stretch bands of CO bound to hemeproteins we perform pressure jump experiments on carbonmonoxy hemeproteins (myoglobin, horseradish peroxidase, chloroperoxidase, P450) in 75% glycerol/water at temperatures from 150 to 210K and pressures from 200 MPa to 0.1 MPa. Several relaxation processes are observed with nonexponential time dependence and non-Arrhenius temperature dependence.

*Supported by HHS PHS 2 ROI GM18051, NIH PHS 2 ROI GM07768-29, PHS 5 ROI GM31756 and NSF DMB82-09616.

⁺permanent address: Central Institute of Molecular Biology of the Academy of Sciences of the GDR, Berlin-Buch, GDR.

Tu-Pos47

RELAXATION OF MbCO IN A GLASS UPON EXTENDED ILLUMINATION

S. D. Luck, A. Ansari, B. R. Cowen, H. Frauenfelder, T. B. Sauke, P. J. Steinbach and R. D. Young. Dept. of Physics, University of Illinois at Urbana-Champaign, 1110 W. Green St., Urbana, IL 61801.

The rebinding of CO to sperm whale myoglobin (Mb) is slowed by extended illumination of the sample (1). The observed "pumping" of the system into long-lived states is well fit by simple one-dimensional diffusion similar to that suggested by Agmon and Hopfield (2,3). The slowed rebinding is caused by diffusion along a protein coordinate perpendicular to the reaction coordinate, but unlike the AH model, our model allows diffusion only during illumination. The pumping data at temperatures between 40 and 140K are thus consistent with a photon-assisted relaxation process.

This work was supported by NIH Grant GM 18051 and S. L. thanks NSERC for a postdoctoral fellowship.

References:

1. A. Ansari *et al.*, Biophys. Chem. 26, 337-355 (1987).
2. N. Agmon and J. J. Hopfield, J. Chem. Phys. 78, 6947-6959 (1983).
3. N. Agmon and J. J. Hopfield, J. Chem. Phys. 79, 2042-2053 (1983).

Tu-Pos49

THE INTERACTION OF SICKLE CELL HEMOGLOBIN POLYMERS WITH CELL MEMBRANES. P. J. Baxter-Rahmoeller and H. Mizukami. Division of Regulatory Biology and Biophysics, Department of Biological Sciences, Wayne State University, Detroit, Michigan, 48202.

We have examined the relationship between the rate of HbS polymer formation and the presence of normal red cell membranes using both embedded and negatively stained specimens with a transmission electron microscope (TEM).

Hemoglobin free ghosts were prepared from the erythrocytes of normal donors in the usual manners, and from these, inside-out vesicles (IOV's) were prepared. Chromatographically pure sickle cell hemoglobin solutions (from donors homozygous for the sickle cell trait) of varying concentrations were mixed with the IOV's, and the suspensions were deoxygenated in a controlled atmosphere glove box for a specific time. The samples with and without IOV's were fixed with glutaraldehyde, and were either negatively stained with phosphotungstic acid, or further processed for embedding and sectioning.

Our observations suggest that though both samples with and without IOV's may form polymers, the samples with IOV's exhibited a significant increase in the population of large HbS polymers. (Supported in part by grants from NIH HL 16008)

Tu-Pos50

MODULATED EXCITATION TESTS OF EQUILIBRIUM MODELS FOR HEMOGLOBIN OXYGEN BINDING AND THE BOHR EFFECT

Mingdi Zhao, Jie Jiang, Nianqing Zhang*, Frank A. Ferrone, & Anthony J. Martino**, Department of Physics and Atmospheric Science, Drexel University, Philadelphia, PA 19104

The method of modulated excitation (Ferrone & Hopfield (1976) *PNAS* 73 4497, Ferrone, Martino, & Basak, (1985) *Biophys. J.* 48 269), by generating allosteric rate pairs, allows the equilibrium between R (relaxed) and T (tense) quaternary structures to be measured. This quantity provides sensitive tests for equilibrium models of oxygen binding. Two cases will be discussed: (1) In a recent expansion of the Szabo-Karplus model, Lee et al. (Lee, Karplus, Poyart & Bursaux (1988) *Biochemistry* 27 1285) found an effective L_3 of 0.06. The experimentally determined value is near unity. (2) Johnson, Turner and Ackers (1984, *PNAS* 81, 1093) have presented an alternative formalism which calls for almost 30% R state with a single ligand bound. In modulated excitation studies of the singly ligated state, we find no evidence for such large contribution of the R state.

*present address: Biophysics Group, 102 Donner Lab, UC Berkeley, Berkeley, CA 94720 **present address: Engineering Physics Laboratory, E. I. DuPont de Nemours & Co., Wilmington, DE 19880-0357.

Tu-Pos52

MONOMER DIFFUSION INTO POLYMER DOMAINS IN SICKLE HEMOGLOBIN

Michael R. Cho and Frank A. Ferrone, Department of Physics and Atmospheric Science, Drexel University, Philadelphia, PA 19104

The gelation of sickle hemoglobin includes the formation of spherulitic arrays of polymers, known as polymer domains, which are an intrinsic result of the polymer formation mechanism. We have observed the diffusion of monomers into domains as they form, which substantially increases the total concentration of hemoglobin within the domain, and, with a half time of tens of seconds, may double the polymer concentration in the center of the domain. The maximum total concentration is somewhat smaller than the pellet concentration obtained in sedimentation experiments, and is slightly dependent on initial concentration and temperature. The rate of approach to the maximum depends on the temperature (25 Kcal/mol activation energy) and the 8th power of the initial concentration. The concentration progress curves analyzed by Singular Value Decomposition, show that all curves have a similar shape and cannot be described by single exponential.

Tu-Pos51

THEORY OF THE SPATIAL GROWTH OF SICKLE HEMOGLOBIN POLYMER DOMAINS.

Huan Xiang Zhou* and Frank A. Ferrone, Department of Physics & Atmospheric Science, Drexel University, Philadelphia, PA 19104.

We have generalized the double nucleation mechanism of Ferrone *et al.* (Ferrone, Sunshine, Hofrichter & Eaton, 1980, *Biophys. J.*, 32, 361; Ferrone, Hofrichter & Eaton, 1985, *J. Mol. Biol.*, 183, 611) to describe the spatial dependence of the radial growth of polymer domains of sickle hemoglobin. Although this extended model requires the consideration of effects such as monomer diffusion, which are irrelevant to a spatially uniform description, no new adjustable parameters are required since diffusion constants are known independently. We find that monomer diffusion into the growing domain can keep the net unpolymerized monomer concentration approximately constant, and in that limit we present an analytic solution. The model shows the features reported by Basak, Ferrone, & Wang, (1988, *Biophys. J.*, 54, 829) and provides a new means of determining the rate of polymer growth. When spatially integrated, the model exhibits the exponential growth seen in other studies. The model developed here can be easily adapted to any spatially dependent polymerization process.

*present address, Laboratory of Chemical Physics, NIH, Bethesda, MD 20892.

Tu-Pos53

ALLOSTERIC KINETICS & EQUILIBRIA DIFFER FOR CO AND O₂ BINDING TO HEMOGLOBIN.

Nianqing Zhang*, Frank A. Ferrone, & Anthony J. Martino**, Department of Physics and Atmospheric Science, Drexel University, Philadelphia, PA 19104

We have used the method of modulated excitation (Ferrone & Hopfield (1976) *PNAS* 73 4497; Ferrone, Martino, & Basak, (1985) *Biophys. J.* 48 269) to measure the forward and reverse rates of the allosteric transition of hemoglobin in pH 7, phosphate buffer between R (relaxed) and T (tense) quaternary structures to which three oxygen molecules were bound. The T structure is favored more strongly in triligated oxyhemoglobin than triligated HbCO. The rates for the allosteric transition with oxygen bound were essentially temperature independent, while for CO both the R→T and T→R rates increased with temperature (activation energy of 2.2 and 2.8 kcal respectively). The R→T rate was higher for O₂ than for CO, viz. $3 \times 10^3 \text{ s}^{-1}$ vs $1.5 \times 10^3 \text{ s}^{-1}$ for HbCO at 18°C. The T→R rate for HbO₂ was only $2 \times 10^3 \text{ s}^{-1}$. The data suggest that there may be some allosteric inequality between the subunits, but do not require (or rule out) ligand binding heterogeneity. The ligand dependent differences are compatible with stereochemical studies of HbCO and HbO₂.

* present address: Biophysics Group, 102 Donner Lab, U C Berkeley, Berkeley, CA 94720 **present address: Engineering Physics Laboratory, E. I. DuPont de Nemours & Co., Wilmington, DE 19880-0357.

Tu-Poe54

LOW TEMPERATURE TIME DEPENDENT RESONANCE RAMAN SPECTRA OF CO BOUND TO SPERM WHALE MYOGLOBIN, Mb AT pH 3: *I E T Iben, J Friedman* (AT&T Bell Labs & NYU (chem)) *B Cowen, H Frauenfelder* (U of Illinois, CU (phys)) and *R Sanches* (U Sao Paulo, Brazil (phys))

Cryogenic samples of MbCO at pH 3 were studied using ns and ps time resolved resonance Raman spectroscopy. Using a 10ns, 423nm, excitation-probe laser pulse, we observed a predominantly CO bound spectrum even at 10K, whereas a pH 7 sample is completely photolyzed. The values of the core markers are similar at pH 3 and pH 7, indicating a 6-coordinated, low-spin species; however, the Fe-CO stretch frequency is decreased from 507cm^{-1} to $\sim 490\text{cm}^{-1}$, revealing a more open heme pocket. Shifting the pulse to 430nm results in an enhanced contribution from the photoproduct population. The relative amplitude of the 10ns photoproduct spectrum decreases with increasing temperature. Despite adequate S/N, the Fe-His(F8) stretch is not observed showing that the Fe-His(F8) bond is broken by 10ns. We also measured the time evolution of the photoproduct Raman spectrum from 30ps to 3ns at 80K and 100K. 50% recombines non-exponentially in time by $\sim 300\text{ps}$, supporting the flash photolysis rebinding data of Cowen et al (1989, Biophys J. 55.M- PM-E11)

Tu-Poe56

THEORY OF LIGHT SCATTERING FROM SMALL SPHERULITIC DOMAINS OF SICKLE HEMOGLOBIN POLYMERS. *J. R. Wheeler* and *Marilyn F. Bishop*, Dept. of Physics, Virginia Commonwealth Univ. 1020 West Main St., Richmond, VA 23284-2000.

We have calculated the light scattering from spherulitic domains of sickle hemoglobin (HbS) polymers, where the domains are well separated and small compared with the wavelength of incident light. Inside a spherulite, we have used a model uniform anisotropic effective medium dielectric tensor. This effective medium is composed of polymers, monomers, and solution, and the anisotropy results from polymer alignment within the domain. Outside the spherulite, we assume an isotropic effective medium composed of monomers and solution. The results depend on the average length of polymers, which we have obtained from the double nucleation mechanism as a function of the extent of polymerization.

This work is supported by NIH Grant Number 38614.

Tu-Poe55

CONFORMATIONAL DISORDER AND REACTIVITY: PHOTODISSOCIATION QUANTUM YIELD STUDIES IN OxyHb(Mb)

M. Chance,² *M. Chavez*,⁴ *S. Courtney*,^{1,3} *J. Friedman*,^{1,3} *M. Ondrias*,⁴ *AT&T Bell Labs*,¹ *Georgetown U*,² *NYU*,³ *U of New Mexico*⁴

Transient absorption studies by several groups suggest that the low quantum yield of photodissociation of O₂Hb(Mb) at ambient temperatures is due to geminate recombination occurring from picoseconds to nanoseconds. We have extended these studies to cryogenic temperatures where we find, using both cw and 30 ps pulses, that a sizable fraction (60% at 8K) of an O₂Hb(Mb) sample can not be photodissociated even with extensive optical pumping. These findings in conjunction with transient absorption measurements with 50 ps resolution, together indicate that at 10K or lower, the low quantum yield is due to a population of conformational substates that undergoes either an ultra fast ($\ll 10\text{ps}$) geminate recombination process or a photophysical process that results in the recovery of the oxy species. Line shape comparisons of the photoproduct absorption in the region of the inhomogeneously broadened band III ($\sim 760\text{nm}$) for CO and O₂ form of Hb(Mb) indicate that the "unphotolyzable" part of the distribution of substates for oxy photoproducts resembles the fast recombining population of carboxy photoproducts observed in kinetic hole burning experiments. A structural model incorporating the iron displacement and the tilt and rotational degrees of freedom of His(F8) is used to explain the mapping of ligand reactivity onto the inhomogeneous line shape of band III.

Tu-Poe57

RESONANCE RAMAN STUDIES OF STEADY STATE HEME REDUCTION AND PHOTOREDUCTION IN CYTOCHROME b₆f and bc₁ COMPLEXES.

*J. D. Hobbs*¹, *R. M. Wynn*², *S. Guner*³, *D. J. Nunez*¹, *R. Malkin*², *D. B. Knaff*³, and *M. R. Ondrias*¹.

1. Department of Chemistry, University of New Mexico, Albuquerque, NM. 2. Division of Molecular Plant Biology, University of California at Berkeley, Berkeley, CA. 3. Department of Chemistry & Biochemistry, Texas Tech University, Lubbock, TX.

The heme sites of the isolated cytochrome b₆f complex in various stages of reduction have been studied using resonance Raman techniques. The spectra are interpreted in terms of Raman spectra for the related bacterial cytochrome bc₁ complex and the isolated turnip cytochrome f. Transient photoreduction behavior of these complexes has been observed using electron transfer inhibitors and oxidation/reduction mediators. Rapid photoreduction of the oxidized heme c₁ and f has been observed in a nanosecond time scale using high laser fluxes. High power 410 nm laser excitation yields a spectrum similar to that observed for the sodium ascorbate reduced complexes. (Supported by NIH GM33330.)

Tu-Pos58

EFFECTS OF PROTEIN ENVIRONMENT ON THE CONFORMATION OF METALLOPORPHYRINS. R.G. Alden, M.R. Ondrias, Dept. of Chemistry, Univ. of New Mexico, Albuquerque, NM 87131. J.A. Shelnutt, Sandia National Laboratories, Albuquerque, NM 87185.

The effects of π - π dimerization and complex formation on the conformations of the macrocycle of nickel(II) uroporphyrin I (NiUrop⁸⁻) have been determined using Raman difference spectroscopy. Both planar and ruffled species coexist in alkaline solution. Formation of the methylviologen π - π complex causes the uncomplexed planar form of NiUrop⁸⁻ to ruffle. These results are compared with similar resonance Raman data for nickel-protoporphyrin human hemoglobin and α -subunits. The active site of the tetramer strongly favors the planar conformation of the macrocycle. However, the presence of a ruffled component of four-coordinate Ni protoporphyrin in the α chains may account for their lowered affinity. This suggests a mechanism for control of axial ligand affinity by modulation of the conformation of the porphyrin. (Supported by the NIH (GM33330) and DOE (DE-AC04-76DP00789).)

Tu-Pos60

TRANSIENT RESONANCE RAMAN INVESTIGATION OF Ni(II)-Fe(II) HYBRID HEMOGLOBINS. M.D. Chavez, S.A. Majumder, P.Y.F. Hsu, D.J. Nunez, M.R. Ondrias, Dept. of Chemistry, Univ. of New Mexico, Albuquerque, NM 87131.

Photoligation behavior of Ni-Fe hybrid hemoglobins has been studied by transient resonance Raman scattering. Our data reveal structural and dynamic features of the α and β subunits of Hb. Both the α and β Ni-subunits exist as equilibria between four and five-coordinate species. The Ni-subunits of $\alpha_2(\text{Ni})\beta_2(\text{FeCO})$ and $\alpha_2(\text{FeCO})\beta_2(\text{Ni})$ displayed photoligation behavior similar to NiHb. The equilibrium structures of the deoxy Fe-subunits were similar to those in the native tetramer, but photodissociation of the CO from the Fe-subunits revealed a $\nu_{\text{Fe-His}}$ indicative of a more T-state structure. The deoxy forms of $\alpha_2(\text{Ni})\beta_2(\text{Fe})$ and $\alpha_2(\text{Fe})\beta_2(\text{Ni})$ favored the formation of four-coordinate Ni sites, yet photoassociative behavior of the proximal histidine was retained. The communication between the α and β chain and its effects on the Ni sites will be discussed in detail. (This work supported by NSF (DMB-8604435), NIH (GM33330) and MBRS (BRS5506RR08139-15).)

Tu-Pos59

RESONANCE RAMAN STUDIES OF NON-COVALENT COMPLEX FORMED BY CYTOCHROME c/CYTOCHROME c PEROXIDASE. Jianling Wang,* Randy W. Larsen,* Susan J. Moench,* James D. Satterlee,# & Mark R. Ondrias* *Dept of Chemistry, University of New Mexico, Albuquerque, NM 87131; #Dept of Chemistry, Washington State University, Pullman, WA 99164. Resonance Raman studies have been carried out on the non-covalent complex formed by cytochrome c (Cyt_c)/cytochrome c peroxidase (CCP) at pH=7.0 and at low ionic strength. ν_3 , the spin-state sensitive mode, of CCP has been monitored to investigate the variations induced by complexation. A 6-coordinated low-spin species has been observed for CCP in the Cyt_c(II)/CCP(III) complex at 1506 cm^{-1} under conditions where tight binding between CCP and Cyt_c is favored, whereas 5-coordinated high-spin species has been detected at 1492 cm^{-1} at high ionic strength as well as for those of the pure ferric CCP(III) at both low and high ionic strength, indicating that the spin-state changes are induced by complexation. These results will be discussed in relation to the function of the Cyt_c/CCP complex. (Supported by the NIH GM33330, NSF PCM DM8 8403353, and CHE 8201374)

Tu-Pos61

ACTIVE SITE CONFORMATION IN MYOGLOBIN AS DETERMINED BY X-RAY ABSORPTION SPECTROSCOPY. K. Zhang, K.S. Reddy, G. Bunker, and B. Chance. Institute for Structural and Functional Studies, and Department of Biochem. and Biophys, University of Pennsylvania Philadelphia, PA 19104

X-ray absorption fine structure experiments were performed to study structural and dynamical aspects of the active site of various forms of myoglobin. The structures determined for Mb, MbCO and MbO₂ are consistent with the structure established by X-ray absorption fine structure experiment and X-ray crystallography. This study focuses on the change of the EXAFS Debye-Waller factor with temperature, which is a measure of thermal and static disorder. It was found that the change of Debye-Waller factor with temperature for the Mb proteins, except Mb, are consistent with a simple Einstein model, in which a single frequency was assumed for the bond stretching modes. In contrast, the temperature dependence of Mb cannot be fitted to the Einstein model and a large disorder was found at the low temperatures, which indicates the existence of conformational substates of the active site.

Tu-Poe82

PROTON INTERACTIONS IN THE RESTING FORM OF CYTOCHROME OXIDASE, by Pavlos Papadopoulos, Scott Walter, and Gary Baker, Department of Chemistry, Northern Illinois University, DeKalb, IL 60115.

The position of the optical Soret band in a dilute solution of cytochrome oxidase was found to reversibly depend on pH. Low pH (6.5-6.7, 20°C) blue shifted the band as far as 415.7 nm, while a titration to high pH (10.0-10.5, 20°C) caused a red shift to 426.9 nm. Intermediate values of pH led to a titration profile that showed a pK_a of 8.6-8.8. During the approach to equilibrium at any pH, an isosbestic point was observed in a series of optical spectra for both blue shifting and red shifting cases. The pH effect on the optical band was found to be an effect on cytochrome a₃³⁺, but no change in spin state, oxidation state, or coordination number could be detected. The blue shift at low pH was accompanied by an increase in absorbance at 415.7 nm while a titration back to high pH caused a decrease. The kinetics of both processes revealed a fast and slow phase. The fast phase was complete within the 2-3 second mixing time for the experiment and accounted for 50% of the total absorbance change. A protonation/deprotonation model involving the histidine of cytochrome a₃³⁺ is proposed.

Tu-Poe84

CHLORIDE DEPLETION OF CYTOCHROME C OXIDASE.

Zhuyin Li and Sunney I. Chan, Noyes Lab. of Chemical Physics 127-72, California Institute of Technology, Pasadena, CA 91125

The strong magnetic interaction between Fe_{a3} and Cu_B in the resting form of cytochrome c oxidase is thought to be mediated by a bridging ligand. The identity of this ligand has been proposed to be an imidazole from a histidine residue, a thiolate sulfur from cysteine, an oxygen from a hydroxide or μ -oxo anion. Earlier EXAFS measurements have implicated either a bridging S or Cl atom. However, a recent EXAFS experiment on a sample of oxidase isolated and purified in Cl⁻-free buffer solutions revealed no (S,Cl) scattering in the Fe EXAFS of the resting oxidase, thus suggesting Cl⁻. To confirm this finding, we have studied samples of reduced oxidase that have been dialyzed against Cl⁻-free buffer in the presence of chelex resin, and have examined the spectroscopic and ligand-binding properties of the reoxidized enzyme. On the basis of optical and EPR measurements, including the effects of ligand-binding (F⁻, Cl⁻, Br⁻ and CN⁻) on these properties of the enzyme, we conclude that the bridging ligand must be Cl⁻ in the resting oxidase.

Tu-Poe83

FRONT-FACE FLUORESCENCE ANALYSIS OF ACID AND ALKALINE DISSOCIATION OF EARTHWORM HEMOGLOBIN, *LUMBRICUS TERRESTRIS*. John P. Harrington, Dept. of Chemistry, Univ. of South Alabama, Mobile, AL and Rhoda Elison Hirsch, Albert Einstein College of Medicine Bronx, N.Y. The steady-state fluorescence properties of the multisubunit structure (dodecamer) of the high molecular weight (3.8x10⁶) earthworm Hb were examined by front-face fluorometry which (1) can provide information about regions rich in aromatic amino acid residues and (2) is sensitive to the aggregated state of Hb. Acid and alkaline dissociation of this Hb were examined over the pH range 3.7-12.5 using different liganded states (oxy, CO, met). We observe (exc. 280nm): (1) intensity of em. max. of oxyHb at acid end point (pH 4.18), 320nm is >> alkaline end point (pH 10.5), 333nm implying different subunit behavior; (2) tyrosinate forms at high pH; (3) rel. intensity of em. max. at 320 nm increases as follows, oxy < deoxy < CO < met at pH 7.0; (4) spectra obtained for oxyHb (pH 10.5) and COHb (pH 7.0) dissociation by 1M MgCl₂ were superimposable suggesting similar subunit dissociation. These findings are consistent with earlier light scattering and CD studies indicating only subunit dissociation up to pH 10.1, with some concurrent unfolding above this pH (Harrington et al., 1973, 1975).

Tu-Poe85

OPTICAL MORPHOLOGY AND NUCLEATION OF SICKLE HEMOGLOBIN GELS. Garrott W. Christoph, James Hofrichter, William A. Eaton. Laboratory of Chemical Physics, NIDDK, NIH, Bethesda, Md. 20892.

When examined between crossed polarizers, deoxyhemoglobin S gels appear as arrays of spherulitic domains. The double nucleation model for the gelation of deoxyhemoglobin S postulates that polymers can be nucleated in the bulk solution phase (homogeneous nucleation) or on the surface of existing polymers (heterogeneous nucleation). As polymerization proceeds, the available surface area increases, increasing the rate of heterogeneous nucleation, thereby providing a mechanism for the autocatalysis that is manifested as the apparent delay in the kinetic progress curve. Homogeneous nucleation of a single polymer triggers the formation of a large number of heterogeneously nucleated polymers. If all the heterogeneously nucleated polymers resulting from a single homogeneous nucleation event are organized into a single spherulitic domain, then the rate of domain formation is equal to the rate of homogeneous nucleation. To test this idea, we have used polarization microscopy to study the domain structure of gels of deoxyhemoglobin S formed at different rates in temperature jump experiments. We find that the density of domains is proportional to about the 35th power of the deoxyhemoglobin S concentration, while, as previously observed, the delay time is inversely proportional to about the 35th power of the concentration. Thus, the rate of domain formation, as calculated from these results, is more sensitive to the concentration than the delay time, supporting the hypothesis that the domain formation rate is equivalent to the rate of homogeneous nucleation. These studies also suggest that differences in intracellular polymerization kinetics, which are preserved as differences in the number of polymer domains, can explain the observed variation in morphology of sickled cells.

Tu-Pos66

KINETICS OF TERTIARY AND QUATERNARY STRUCTURAL CHANGES IN HEMOGLOBIN. A. Ansari, C. M. Jones, E. R. Henry, J. Hofrichter, W. A. Eaton, Laboratory of Chemical Physics, NIDDK, NIH, Bethesda, MD 20892; and T. Yonetani, Department of Biochemistry and Biophysics, U. of Pennsylvania, Phila., PA 19104.

A detailed description of the kinetics of tertiary and quaternary conformational changes remains a major problem in protein physical chemistry. To investigate this problem we have used time-resolved absorption spectroscopy to explore the kinetics of the hybrid hemoglobin molecule in which cobalt has been substituted for the heme iron in the α chains. Carbon monoxide binds cooperatively to the β hemes but does not bind to the cobalt porphyrins. This molecule thus provides a simplified system for studying ligand binding and conformational changes following photodissociation of the carbon monoxide complex. From the dependence of the observed kinetics on the degree of photolysis, we can obtain separate progress curves for the unliganded and singly liganded photoproduct species. The kinetics of bimolecular rebinding to the singly liganded molecule exhibit two rapid relaxations, which can be explained in terms of the two-state allosteric model by postulating that ligand binding and switching between the R_1 and T_1 quaternary structures occur on the same time scale. Analysis of this progress curve yields rates for the $R_1 \Rightarrow T_1$ and $T_1 \Rightarrow R_1$ quaternary transitions which are both about $3 \times 10^9 \text{ s}^{-1}$. The kinetics of the deoxyheme spectral changes confirm these assignments. The results for the unliganded molecule are more complex because tertiary relaxation appears to be incomplete prior to the $R_0 \Rightarrow T_0$ quaternary transition. The $R_0 \Rightarrow T_0$ rate is between 10- and 50-fold greater than the $R_1 \Rightarrow T_1$ rate; its precise determination is dependent upon the model used to describe the properties of the unrelaxed R_0 molecule.

Tu-Pos68

LINKAGE GRAPHS OF CO AND O₂ BINDING TO HEMOGLOBIN A₀.

Mauro Angeletti, Joe Simmons, and Stanley J. Gill

Department of Chemistry and Biochemistry,
University of Colorado, Boulder CO, 80309-0215.

For hemoglobin the binding of the two gaseous ligands, O₂ and CO, is identically linked since binding occurs competitively to the same site. The fundamental thermodynamic properties of the binding process are revealed by binding curves and the derivatives of such curves. The effect of linkage between two ligands can be displayed by three dimensional graphs which have a basic thermodynamic origin in the binding potential and its Legendre transformations. The first derivatives of these functions yield binding curves under various specified conditions that correspond to open and closed systems. The second derivatives display the cooperativity (binding capacity) and stoichiometric linkage (Bohr coefficient) features of the system under various conditions. These features are conveniently represented in terms of Hill coefficients and a normalized degree of linkage parameter. We wish to illustrate some of the general features of linkage graphs for O₂ and CO binding to HbA₀ by three dimensional linkage graphs for open and closed conditions.

This work was supported by NIH Grant HL 22325.

Tu-Pos67

THE EFFECT OF pH ON THE STRUCTURE OF ALPHA APOHEMOGLOBIN MEASURED BY STEADY-STATE FLUORESCENCE ENERGY TRANSFER. Shawn M. O'Malley* and Melisenda J. McDonald, Biochemistry Program, Department of Chemistry, University of Lowell, Lowell MA 01854.

The sole tryptophan donor (residue 14) of normal human hemoglobin alpha globin chains prepared by acid-acetone method was excited at 290 nm and emission spectra (300-400nm) were recorded on an SLM/AMINCO spectrofluorometer temperature regulated at 5°. Fluorescence monitoring of alpha globin chains labeled with an acceptor group at the 104 cysteine position with a novel non-fluorescent sulfhydryl reagent, 4-phenylazophenylmaleimide (Molecular Probes) demonstrated energy transfer between donor and acceptor. The ratio of fluorescence intensity of labeled to unlabeled globin increased over a pH range 8.0 to 6.5 (0.05 M potassium phosphate buffer) indicating a decrease in efficiency of energy transfer with addition of protons. This decrease apparently corresponds to an expansion of the alpha globin structure (an average distance change between donor and acceptor of approximately 5 Angstroms). This pH effect may be related to electrostatic interactions which govern hemoglobin subunit assembly. Furthermore, preliminary static studies show comparable quenching of fluorescence emission of labeled and unlabelled alpha chains upon addition of beta heme chains. Stopped-flow fluorescent measurements with normal and variant beta heme chains are planned. Supported by NIH Grant HL 38456.

Tu-Pos69

NON-LINEAR OPTICAL EFFECTS IN OXYGEN BINDING REACTIONS OF HUMAN HBA₀

D.W. Ownby and S.J. Gill, Dept. of Chemistry and Biochemistry, University of Colorado, Boulder, Co., 80309

Abstract: Application of the matrix method of singular value decomposition (SVD) to the oxygen binding reaction of human HbA₀ has confirmed the presence of significant optical non-linearity in the Soret band (440-400 nm). A spectra is collected over the full wavelength range at each of several oxygen partial pressures spanning the oxygen binding region. SVD analysis of the resulting matrix has shown that there are at least two optically distinct transitions present. Simultaneous fitting of the different wavelengths to an Adair type equation, as well as the transitions recovered from the SVD analysis, have shown that the data is best represented by a modified Adair equation in which the change in optical density per heme is 5-10% less in the first and second ligation steps than in the third and fourth.

Supported by NIH Grant HL 22325.

Tu-Pos70

STABILIZATION OF THE T-STATE OF HEMOGLOBIN

Stanley J. Gill, Michael L. Doyle, and Joe H. Simmons

Department of Chemistry and Biochemistry,
University of Colorado, Boulder, Colorado 80309-0215

The effect of inositol hexaphosphate and bezafibrate on binding of O₂ and CO to HbA₀ at high concentrations (1 mM) has been evaluated using thin layer optical techniques. Data analysis shows 1) the occurrence of greatly reduced ligand dependent cooperativity (Hill slope of 2.23 for CO and 1.51 for O₂), and 2) the presence of significant triply ligated species. The data fits a nested allosteric two-state MWC model in which the T state consists of two allosteric substates, T_i and T_r, where T_i binds only to the α chains and T_r binds to both α and β chains. The model indicates that the triply ligated species consists of a predominant amount of T form, agreeing with kinetic observations of CO ligated hemoglobin. The maximum amount of triply ligated R molecules (CO or O₂) implicated is less than 1%, a result similar to that found previously for binding studies made in the absence of BZF and IHP.

Supported by NIH grant HL 22325

Tu-Pos72

EPR OF MYELOPEROXIDASE AND ITS LIGAND COMPLEXES

H. Caroline Lee**, Karla S. Booth*, Winslow S. Caughey* and Masao Ikeda-Saito**

**Univ. of Penn., Phila., PA 19104 and Case Western Reserve Univ., Cleveland, OH 44106; *Colorado State Univ., Fort Collins, CO 80523

High spin resting myeloperoxidase and halide complexes showed pH-dependent EPR spectral changes with two distinct pK's. Halide concentrations also affected the relative intensities of the acid, neutral and alkaline forms of halide complexes. Acid-neutral transitions were observed for low spin nitrite and azide adducts, with pK's less than 4 and near 6, respectively; whereas EPR of cyanide adduct was independent of pH. Halides induced spectral changes in low spin cyanide complexes at acidic, neutral and alkaline pH's. The pH and halide effects on EPR of myeloperoxidase are considered to be modulated by two distal ionizable groups.

(supported by N.I.H. grants GM39492 and HL15980)

Tu-Pos71

EPR STUDIES OF PHOTOLYSIS OF HbNO AT LOW TEMPERATURES--*Marília P. Linhares, Léa J. El-Jaick, George Bemski and Eliane Wajnberg - Centro Brasileiro de Pesquisas Físicas - Rua Dr. Xavier Sigaud, 150-Urca - CEP 22290 - Rio de Janeiro-RJ - *Instituto de Física-Universidade Federal do Rio de Janeiro-Brasil

Photolysis of R-state nitroxide-human hemoglobin (0.2mM Fe) has been studied from 6.2K to 15.5K by electron spin resonance during and after continuous illumination. Non exponential kinetic of both dissociation and reassociation of NO was observed. The extended illumination separates the fast from the slower ligands. In order to analyse the temperature dependence of the reassociation rate at low temperatures our experimental kinetic curves were fitted with a sum of two exponentials. Normalized kinetic curves were also fitted with the energy distribution in the conformational substates model, under the hypothesis of recombination via quantum mechanical tunneling. This model yields 4.94 kJ/mol for the peak energy and 3.25 for the logarithm of the frequency factor.

Tu-Pos73

A PERTURBED "R" STATE RESPONSIBLE FOR HEMOGLOBIN OXIDATION. L. Zhang, J.M. Rifkind, and A. Levy. NIH/NIA, Gerontology Research Center, Baltimore, Maryland 21224.

The rate of autoxidation of hemoglobin has been studied as a function of oxygen pressure and heme concentration. It has been previously observed that lowering the oxygen pressure of hemoglobin results in an enhanced rate of oxidation. These studies have generally been attributed to the oxidative instability of T-state hemoglobin. Our detailed studies confirm that fully oxygenated tetrameric hemoglobin is particularly resistant to oxidation. However, the partially liganded T-state hemoglobin with one oxygen bound is oxidized only slightly faster. The major source for hemoglobin oxidation is tri-liganded, predominantly R-state, hemoglobin. The instability of the perturbed R-state is further confirmed by concentration studies which indicate a 25-fold greater rate of oxidation for fully liganded dimer than fully liganded tetramer. Studies with valency hybrids indicate a mechanism whereby conformational perturbation associated with an unoccupied ligand pocket are transmitted between hemes in the R-state across the $\alpha_1\beta_1$ interface.

Tu-Pos74**THE THERMODYNAMIC LINKAGE BETWEEN DIMER-TETRAMER ASSEMBLY AND OXYGENATION OF COBALT SUBSTITUTED HEMOGLOBIN.**

P.C. Speros*, M.L. Doyle*, V.J. LiCata*, D. Gingrich*, B.M. Hoffman*, and G. K. Ackers.*

*Department of Biology, The Johns Hopkins University, Baltimore, MD 21218

*Department of Chemistry and Department of Biochemistry, Molecular and Cell Biology, Northwestern University, Evanston, IL

Cobalt substituted hemoglobin binds oxygen reversibly, cooperatively and in full response to allosteric effectors. Assembly of unligated and fully oxygenated hemoglobin dimers into tetramers is energetically linked to the respective oxygenation of dimers and tetramers. The assembly free energy of deoxy-dimers into deoxy-tetramers has been studied by dissociation and reassociation kinetics, and found to be -10.6 kcal/mol for cobalt hemoglobin.

The determination of median ligand concentrations for the process of saturation by oxygen of cobalt hemoglobin has been performed over a range of concentrations. This information is sufficient to resolve the overall free energies of ligation and the assembly of oxy-dimers into oxy-tetramers. The free energy of fully loading a dimer with oxygen is -11.4 kcal/mol. That for a tetramer is -20.1 kcal/mol. The assembly free energy of oxy-dimers into oxy-tetramers is -7.75 kcal/mol. Therefore, in cobalt hemoglobin, -2.75 kcal/mole of cooperative free energy is expended during the oxygenation process

Tu-Pos76**MOLECULAR COMMUNICATION ACROSS THE REGULATORY INTERFACE IN HUMAN HEMOGLOBIN OPERATES VIA THREE DISTINCT COUPLING MODES.** Vince J. LiCata and Gary K. Ackers, Department of Biology, The Johns Hopkins University, Baltimore, MD 21218.

Long range energetic communication is a key feature of allosteric systems. Cooperative ligation in human hemoglobin has long served as an excellent model system for elucidating general principles of energy transduction within allosteric proteins.

Regulation of ligand binding affinity in this system is due to free energy changes arising from interactions at the $\alpha^1\beta^2$ interface. Cooperative ligation requires energetic communication across this interface, between the two dimers. By determining the relative cooperative free energies of hybrid molecules which simultaneously have structural perturbations at various combinations of the hemes and at sites within the $\alpha^1\beta^2$ interface, one may dissect the nature of the energetic communication across this interface.

Studies of these mutant valency hybrid hemoglobins have provided evidence for three distinct communicative networks within the $\alpha^1\beta^2$ interface. There appears to be a hierarchical organization to the networks. All interfacial residue sites examined are involved in a cooperativity-linked global conformational change. Within the context of this global "pathway" there exist two different types of specific long range communication. One of these classes of specific long range pathways is linked to cooperative ligand binding while the other class is not. The detailed structural and energetic basis of these effects is not yet known.

Tu-Pos75**MOLECULAR SWITCHING IN HUMAN HEMOGLOBIN; THE Co(II)/Fe(II)-CO LIGAND ANALOGUE SYSTEM.**

P.C. Speros*, V.J. LiCata*, T. Yonetani*, and G. K. Ackers.*

*Department of Biology, The Johns Hopkins University, Baltimore, MD

*Department of Biochemistry and Biophysics, University of Pennsylvania School of Medicine, Philadelphia, PA

In order to understand "cooperative switching" in human hemoglobin, one must study the cooperative free energy levels of the low abundance intermediate ligation species. In this study, unligated cobalt substituted heme sites are combined into the same tetramer with naturally occurring iron sites ligated with carbon monoxide, generating the ten structurally-unique combinations of ligated and unligated subunits. Many of the species in this system have been characterized in terms of their dimer-tetramer assembly free energy. Using the thermodynamic linkage between assembly and ligation processes, the experimentally resolved assembly free energy of each ligation species was used to determine the corresponding cooperative free energy.

The patterns of cooperative free energy expenditure among the intermediate species of this system are different from those seen in previously studied ligand analogue systems. These patterns exhibit characteristics implied by or observed in the oxygenation of hemoglobin, including unequal partitioning of the cooperative free energy and quaternary enhancement.

Tu-Pos77**DYNAMICS OF LIGAND RECOMBINATION IN SITE SPECIFIC MUTANTS OF HUMAN MYOGLOBIN.**

D.G. Lambricht, S. Balasubramanian, & S.G. Boxer, Dept. of Chem., Stanford University, Stanford, CA 94305.

J.W. Petrich, J.-C. Lambrich, & J.-L. Martin, Lab. d' Opt. Appl., Ecole Polytech., ENSTA, INSERM U275, 91128 Palaiseau Cedex, France.

Site specific mutants of human Mb have been prepared at Val68, His64, Lys45, and Asp60. Geminate recombination in MbCO and MbNO as well as on- and off-rates for MbCO have been measured in aqueous solution at room temperature. The kinetics for both ligands are very sensitive to substitutions at Val68 (Leu, Ile, Ala, Asn) and His64 (Gln, Ala). The yield and rate of the geminate process increase as the volume of the residue at position 68 decreases. Substitutions at Lys45 (Arg, Gln, Ala) and Asp60 (Glu, Ala) perturb the kinetics for MbCO to a rather small degree. In particular, the Gln and Ala mutants at residue 45 are remarkably similar to wild type, while the Arg mutant exhibits a 2 fold increase in geminate yield. This increase accounts nearly quantitatively for the observed changes in on- and off-rates. It appears that Lys45 and Asp60 do not contribute significantly to the rate determining barriers for diffusion of CO between the solvent and ligand binding site at room temperature. Supported by NIH.

Tu-Pes78

ESR AND ENDOR STUDIES OF METALLOPORPHYRIN
CATION RADICAL MODELS FOR HRP AND CATALASE
COMPOUND I INTERMEDIATES

P.O. Sandusky, W.A. Oertling, C.K. Chang
and G.T. Babcock

Department of Chemistry, Michigan State
University, East Lansing, MI 48824

Two classes of beta-substituted metallo-
porphyrin cation radicals are distinguish-
able; those with optical spectra similar
to that of HRP I and those with optical
spectra similar to Catalase I. Character-
ization of these model species with
respect to meso-proton and nitrogen
hyperfine couplings indicate that both
classes have $^2A_{1u}$ ground states.

Tu-Pos79

TREHALOSE LINKAGE CONFORMATION FROM OPTICAL ROTATION. Christopher A. Duda and Eugene S. Stevens, Department of Chemistry, State University of New York, Binghamton, New York 13901

Trehalose (α -D-glucopyranosyl (1 \rightarrow 1)- α -D-glucopyranoside) apparently has several important biological functions. One of the most recently discovered, with potential biotechnological importance, is its effectiveness in stabilizing membrane structure in the dry state, and perhaps in inhibiting biological damage at low temperatures. It is known that trehalose binds to the head group of lipids in bilayers. Speculation concerning its cryobiological activity has focused on hydroxyl group orientation and the disaccharide linkage conformation.

With a recently developed calculational model for disaccharide optical activity (*J. Am. Chem. Soc.* 1989, 111, 4149), we have found that the observed molar rotation of trehalose (680 deg cm² dmol⁻¹) is what is expected for a linkage conformation near $\phi, \psi = -60^\circ, -60^\circ$. Other energetically allowed conformations are expected to display significantly less optical rotation. The conformation indicated by our analysis has both ring oxygen atoms and both hydroxymethyl groups in general proximity, in contrast with other energetically allowed conformations.

Tu-Pos80

CONFORMATIONAL STUDIES OF OLIGOSACCHARIDES FROM LONG RANGE ^1H - ^{13}C COUPLING CONSTANTS MEASURED BY ^1H DETECTION

Zhen-Yi Yan and C. Allen Bush Dept. of Chemistry and Biochemistry, University of Maryland Baltimore County, Baltimore, MD 21228 U.S.A.

Long range ^1H - ^{13}C coupling constants across glycosidic bond provide valuable information in oligosaccharide conformations. Although we were able to use the ^{13}C detected 2-D proton selective J_{CH} method of Bax and Freeman for measuring the vicinal couplings in natural abundance on the trisaccharide, Man α -(1 \rightarrow 3)Man β -(1 \rightarrow 4)GlcNAc, on a 50 mg sample, the number of oligosaccharides and glycopeptides accessible to this $^3J_{CH}$ measurement is limited by the problem of sensitivity due to ^{13}C detection and the requirement for a separate 2-D spectrum for each proton of interest. To measure $^3J_{CH}$ for a wide range of oligosaccharide samples, we have applied proton detected 2-D heteronuclear correlation spectroscopy. The distorted cross peak multiplets in the phase sensitive HMBC spectrum are analysed with a simple data fitting procedure to extract the values of long range ^1H - ^{13}C coupling constants. The advantages of this experiment are the dispersion of the peaks in 2-dimension ($\delta\ ^1\text{H}$, $\delta\ ^{13}\text{C}$) and the substantially improved sensitivity as a consequence of ^1H detection. These $^3J_{CH}$ are related to glycosidic dihedral angles ϕ and ψ by a Karplus-type curve, and the resulting conformation can be compared to models based on ^1H NOE and energy calculations to determine if a oligosaccharide exists in single or multiple conformations. Research supported by NIH grant GM 31449